AMERICAN SOCIETY FOR MICROBIOLOGY | Journal of Virology®

VACCINES AND ANTIVIRAL AGENTS

Adjuvanting a Simian Immunodeficiency Virus Vaccine with Toll-Like Receptor Ligands Encapsulated in Nanoparticles Induces Persistent Antibody Responses and Enhanced Protection in TRIM5α Restrictive Macaques

Sudhir Pai Kasturi,[a] Pamela A. Kozlowski,[b] Helder I. Nakaya,[a,c] Matheus C. Burger,[c] Pedro Russo,[c] Mathew Pham,[a] Yevgeniy Kovalenkov,[a] Eduardo L. V. Silveira,[a,c] Colin Havenar-Daughton,[d] Samantha L. Burton,[a] Katie M. Kilgore,[a] Mathew J. Johnson,[a] Rafiq Nabi,[b] Traci Legere,[a] Zarpheen Jinnah Sher,[a] Xuemin Chen,[e] Rama R. Amara,[a,f] Eric Hunter,[a,g] Steven E. Bosinger,[a] Paul Spearman,[a,e] Shane Crotty,[d] Francois Villinger,[a,h] Cynthia A. Derdeyn,[a,g] Jens Wrammert,[a,e] Bali Pulendran[a,g]

Emory Vaccine Center/Yerkes National Primate Research Center at Emory University, Atlanta, Georgia, USA[a]; Department of Microbiology, Immunology, and Parasitology, Louisiana State University Health Sciences Center, New Orleans, Louisiana, USA[b]; Faculty of Pharmaceutical Sciences, Department of Clinical and Toxicological Analyses, University of Sao Paulo, Sao Paulo, Brazil[c]; Division of Vaccine Discovery, La Jolla Institute of Allergy and Immunology, La Jolla, California, USA[d]; Department of Pediatrics, Emory University School of Medicine, Atlanta, Georgia, USA[e]; Division of Microbiology and Immunology, Emory University, Rollins Research Center, Atlanta, Georgia, USA[f]; Department of Pathology and Laboratory Medicine, Atlanta, Georgia, USA[g]; New Iberia Research Center, University of Louisiana Lafayette, New Iberia, Louisiana, USA[h]

ABSTRACT Our previous work has shown that antigens adjuvanted with ligands specific for Toll-like receptor 4 (TLR4) and TLR7/8 encapsulated in poly(lactic-co-glycolic) acid (PLGA)-based nanoparticles (NPs) induce robust and durable immune responses in mice and macaques. We investigated the efficacy of these NP adjuvants in inducing protective immunity against simian immunodeficiency virus (SIV). Rhesus macaques (RMs) were immunized with NPs containing TLR4 and TLR7/8 agonists mixed with soluble recombinant SIVmac239-derived envelope (Env) gp140 and Gag p55 (protein) or with virus-like particles (VLPs) containing SIVmac239 Env and Gag. NP-adjuvanted vaccines induced robust innate responses, antigen-specific antibody responses of a greater magnitude and persistence, and enhanced plasmablast responses compared to those achieved with alum-adjuvanted vaccines. NP-adjuvanted vaccines induced antigen-specific, long-lived plasma cells (LLPCs), which persisted in the bone marrow for several months after vaccination. NP-adjuvanted vaccines induced immune responses that were associated with enhanced protection against repeated low-dose, intravaginal challenges with heterologous SIVsmE660 in animals that carried TRIM5α restrictive alleles. The protection induced by immunization with protein-NP correlated with the prechallenge titers of Env-specific IgG antibodies in serum and vaginal secretions. However, no such correlate was apparent for immunization with VLP-NP or alum as the adjuvant. Transcriptional profiling of peripheral blood mononuclear cells isolated within the first few hours to days after primary vaccination revealed that NP-adjuvanted vaccines induced a molecular signature similar to that induced by the live attenuated yellow fever viral vaccine. This systems approach identified early blood transcriptional signatures that correlate with Env-specific antibody responses in vaginal secretions and protection against infection. These results demonstrate the adjuvanticity of the NP adjuvant in inducing persis-

Received 13 September 2016 **Accepted** 23 November 2016

Accepted manuscript posted online 7 December 2016

Citation Kasturi SP, Kozlowski PA, Nakaya HI, Burger MC, Russo P, Pham M, Kovalenkov Y, Silveira ELV, Havenar-Daughton C, Burton SL, Kilgore KM, Johnson MJ, Nabi R, Legere T, Sher ZJ, Chen X, Amara RR, Hunter E, Bosinger SE, Spearman P, Crotty S, Villinger F, Derdeyn CA, Wrammert J, Pulendran B. 2017. Adjuvanting a simian immunodeficiency virus vaccine with Toll-like receptor ligands encapsulated in nanoparticles induces persistent antibody responses and enhanced protection in TRIM5α restrictive macaques. J Virol 91:e01844-16. https://doi.org/10.1128/JVI.01844-16.

Editor Jae U. Jung, University of Southern California

Address correspondence to Bali Pulendran, bpulend@emory.edu.

tent and protective antibody responses against SIV in RMs with implications for the design of vaccines against human immunodeficiency virus (HIV).

IMPORTANCE The results of the RV144 HIV vaccine trial, which demonstrated a rapid waning of protective immunity with time, have underscored the need to develop strategies to enhance the durability of protective immune responses. Our recent work in mice has highlighted the capacity of nanoparticle-encapsulated TLR ligands (NP) to induce potent and durable antibody responses that last a lifetime in mice. In the present study, we evaluated the ability of these NP adjuvants to promote robust and durable protective immune responses against SIV in nonhuman primates. Our results demonstrate that immunization of rhesus macaques with NP adjuvants mixed with soluble SIV Env or a virus-like particle form of Env (VLP) induces potent and durable Env-specific antibody responses in the serum and in vaginal secretions. These responses were superior to those induced by alum adjuvant, and they resulted in enhanced protection against a low-dose intravaginal challenge with a heterologous strain of SIV in animals with TRIM5a restrictive alleles. These results highlight the potential for such NP TLR L adjuvants in promoting robust and durable antibody responses against HIV in the next generation of HIV immunogens currently being developed.

KEY WORDS SIV, vaccine, rhesus macaques, TLR ligands, adjuvants, HIV vaccines, antibody responses, plasma cells, plasmablasts

Despite more than 3 decades of research since the discovery of human immunodeficiency virus type 1 (HIV-1), an AIDS vaccine remains elusive (1, 2). Initial strategies in HIV-1 vaccine development focused on the stimulation of antibody responses using the recombinant monomeric envelope (Env) gp120 protein immunogen (2). Subsequent strategies, such as the recombinant adenovirus type 5 (rAd5) vector approach, focused on eliciting antigen-specific $CD8^+$ T cell responses (1). However, both strategies failed to demonstrate protection in clinical trials, and in fact, the rAd5 approach was reported to result in an enhancement of infection (3). Recently, a phase III clinical trial (the RV144 trial) of a vaccine reported that it yielded modest protective efficacy (~31%) (2, 4). Vaccination with isotype class-switched IgG antibodies specific to the V1/V2 region of HIV-1 gp120 correlated with a decreased risk of infection which waned with time, and vaccination with isotype class-switched IgA antibodies correlated with an increased risk of infection, highlighting a critical balance between the presence of IgG and IgA antibodies in the circulation (5). These results highlight the need to develop vaccines that induce antibody responses of potent magnitude and of a sufficient durability to protect against infection.

The induction of a strong and durable antibody response to vaccination is critically dependent on the use of effective adjuvants that stimulate the innate immune system (6, 7). Recent work in mice, nonhuman primates (NHPs), and humans has highlighted a new generation of molecular adjuvants targeted to pathogen recognition receptors (PRRs) on innate cells, such as dendritic cells (DCs) (8–11). Specific agonists of the Toll-like receptor (TLR) hold much promise as vaccine adjuvants. These adjuvants have, in fact, been licensed for clinical use and have been used in one of the vaccines against human papillomavirus. They are also being evaluated for use in other vaccine regimens against infections and cancers (8). Napolitani and colleagues demonstrated that specific combinations of TLR ligands induced a synergistic activation of cytokine production in human DCs *in vitro* (12). Consistent with this, our recent work demonstrated that the delivery of a specific combination of TLR ligands encapsulated in nanoparticles (NPs) with antigens induced enhanced DC activation and a synergistic increase in antigen-specific T cell and antibody responses in mice (13). A striking result to emerge from this study was that specific combinations of TLR ligands induced a greatly enhanced antibody response and long-lived germinal center (GC) responses similar to those observed in live viral infections (14). The observation that specific combinations of TLR ligands enhance antibody responses has been confirmed by recent studies (15–17).

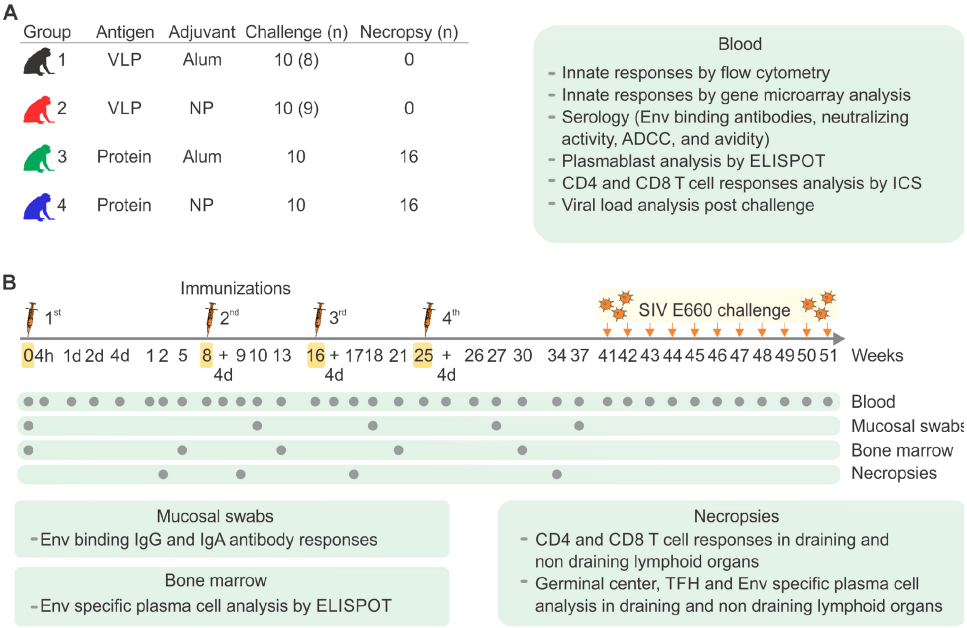

FIG 1 Experimental protocol and schematic. (A) Experimental protocol. Forty female RMs were distributed into four experimental groups. Two animals in group 1 and one animal in group 2 were withdrawn from the study for reasons unrelated to the immunizations. An additional 16 animals were allocated to groups 3 and 4 to investigate the vaccine-specific responses in the draining and nondraining lymphoid organs. Animals in groups 1 and 2 received VLPs consisting of 50 μg of SIVmac239 Env and 1.5 mg of Gag with alum and NP adjuvants, respectively. Animals in groups 3 and 4 received 50 μg of gp140 SIVmac239 Env and 50 μg of recombinant SIVmac239 Gag p55 with alum and NP adjuvants, respectively. (B) Immunization, bleed, and challenge schedule are detailed as shown in the experimental schematic. Animals were bled ~4 weeks before primary immunization for baseline analysis of serological and cellular immune responses. Animals were immunized 4 times at weeks 0, 8, 16, and 25. Animals were rested for 4 months and subjected to a series of challenges with 20,000 $TCID_{50}$ (0.5 to 1.0 AID_{50}) every week for 12 weeks. The innate responses to vaccination were investigated (flow cytometry and transcriptomics) for the first 2 weeks after the primary immunization, and adaptive responses (serological, B cell, and T cell responses) were investigated after each round of immunization. The closed circles in the experimental schematic highlighting necropsies indicate the time points at which 4 animals from groups 3 and 4 were sacrificed to investigate vaccine-specific responses in the draining and nondraining lymphoid organs. Individual treatment group-specific results are color coded consistently throughout the graphs in the figures. n, number of RMs; ADCC, antibody-dependent cell-mediated cytotoxicity; d, day.

These studies highlight the potential of NP-encapsulated TLR ligands to be vaccine adjuvants. In order to demonstrate this preclinically in an NHP model, we evaluated the immunogenicity of two distinct forms of simian immunodeficiency virus (SIV) strain SIVmac239 Env immunogens, a soluble Env protein form and a virus-like particle (VLP) form, each of which was administered with NP and alum adjuvants to rhesus macaques (RMs). Our data demonstrate that when the NP adjuvant is used with soluble Env, it induces robust and durable Env-specific antibody responses in serum and mucosal secretions that correlate with enhanced protection against an SIVsmE660 mucosal challenge. Furthermore, systems-based approaches delineated the novel molecular signatures associated with the enhanced immunogenicity and efficacy of the NP-adjuvanted vaccines.

RESULTS

Experimental design. Animals were allocated to four treatment groups, as described in Fig. 1A. Animals in groups 1 and 2 were immunized with an SIVmac239 VLP that contained Env (50 μg) and Gag (1,500 μg) mixed with the alum or NP adjuvant, respectively. Animals in groups 3 and 4 were immunized with a combination of SIVmac239-derived Env (50 μg) and Gag (50 μg) with alum or NP adjuvant, respectively. For brevity, here we refer to the treatments for groups 1 and 2 as VLP-NP and VLP-alum, respectively, and the treatments for groups 3 and 4 as protein-NP and protein-alum, respectively. Animals carrying either restrictive or permissive TRIM5α alleles were

equally distributed in the treatment groups used in the study, as shown in Table S1 in the supplemental material. VLP integrity was assessed using transmission electron microscopy, and the amounts of Env as well as Gag in VLPs were quantified as shown in Fig. S1 and as described previously (18, 19). Due to the intrinsic stoichiometry of the Env and Gag amounts assembled in VLPs, the dose of Gag was 30-fold higher in groups 1 and 2 than groups 3 and 4. The NP adjuvant doses administered to the RMs (50 μg monophosphoryl lipid A [MPL], 750 μg TLR7/8 ligand R848) were those reported earlier (13), and alum was used at 500 μg following guidelines on the use of alum for preclinical evaluations (20–22). The timing of the vaccinations and immunological analyses is detailed in Fig. 1B.

NP-adjuvanted vaccines induce robust and persistent systemic antibody responses. The magnitude of the binding antibody response against SIVmac239 Env in serum was measured by enzyme-linked immunosorbent assay (ELISA) (Fig. 2A). Env-specific IgG responses were detected at 2 and 5 weeks after the primary immunization and were significantly boosted in all treatment groups after the second immunization. The resulting change in the magnitude of the antibody response at week 10 equaled 227-fold (protein-NP, Wilcoxon matched-pair signed-rank test, $P = 0.0020$), 147-fold (VLP-NP, $P = 0.0039$), 192-fold (VLP-alum, $P = 0.0078$), and 69-fold (protein-alum, $P = 0.0020$) in comparison with that at week 5. The overall response in the study peaked at week 27 (2 weeks after the final vaccination) and was significantly greater in animals vaccinated with protein-NP (titer, 680.77 μg/ml) than in animals vaccinated with (i) VLP-alum (titer, 19.81 μg/ml, 34.4-fold higher; $P < 0.001$, Kruskal-Wallis test followed by Dunn's correction), (ii) VLP-NP (titer, 78.71 μg/ml, ~8.6-fold higher; $P < 0.01$), and (iii) protein-alum (titer, 104.47 μg/ml, 6.5-fold higher; *P* was not significant). At week 41, the responses in animals vaccinated with protein-NP persisted at higher levels (titer, 37.24 μg/ml) than in animals vaccinated with (i) VLP-alum (titer, 1.81 μg/ml, 20.5-fold higher; $P < 0.0001$, Kruskal-Wallis test followed by Dunn's correction), (ii) VLP-NP (titer, 7.32 μg/ml, 5.1-fold higher; *P* was not significant), and (iii) protein-alum (titer, 7.95 μg/ml, 4.7-fold higher; *P* was not significant) (Fig. 2A). The binding antibody responses induced by the NP adjuvant contracted 11-fold and 18-fold when VLP and protein immunogens were used, respectively, and 11-fold and 13-fold contractions from the peak responses were observed when alum adjuvant was used with VLP and protein immunogens, respectively. Furthermore, protein-NP immunization induced higher antibody responses against the Env protein gp140 derived from the SIVsmE660 heterologous challenge virus (titer, 15.24 μg/ml) than those induced by immunization with (i) VLP-alum (titer, 1.78 μg/ml; $P < 0.0001$, Kruskal-Wallis test followed by Dunn's correction), (ii) VLP-NP (titer, 4.87 μg/ml; *P* was not significant), and (iii) protein-alum (titer, 3.91 μg/ml; $P < 0.05$) (Fig. 2B). Homologous Env-specific serum IgA responses were approximately 200-fold lower than the IgG responses but followed kinetics similar to those of the IgG responses, and IgA persisted at higher levels in animals that received protein-NP than in the other groups (Fig. S2A). At week 37 (4 weeks prior to challenge), persistent binding antibody responses capable of recognizing SIVsmE660 gp120 (Fig. 2C) and HIV-2 gp36, a protein that is highly homologous to SIVgp41 (Fig. 2D), were also observed.

Antibody effector functions are dependent on the antibody isotypes as well as glycosylation patterns (23), which could contribute to protective immunity (24). To assess the quality of the antibody responses, we measured antibody-dependent phagocytic (ADP) responses (25). Consistent with the binding antibody responses, there was a significantly enhanced and persistent ADP response in animals immunized with protein relative to that in animals immunized with VLPs (Fig. 2E). Interestingly, similar to the binding antibody responses, higher neutralizing activity against tier 1 SIVsmE660.11 was observed in the serum of animals immunized with protein-NP than in the serum of animals in the other groups (Fig. 2F). However, negligible neutralization of the challenge stock of SIVsm660 was observed in all vaccine groups (Fig. S2B). These data demonstrate that the NP adjuvant enhances humoral immunity against SIV immunogens.

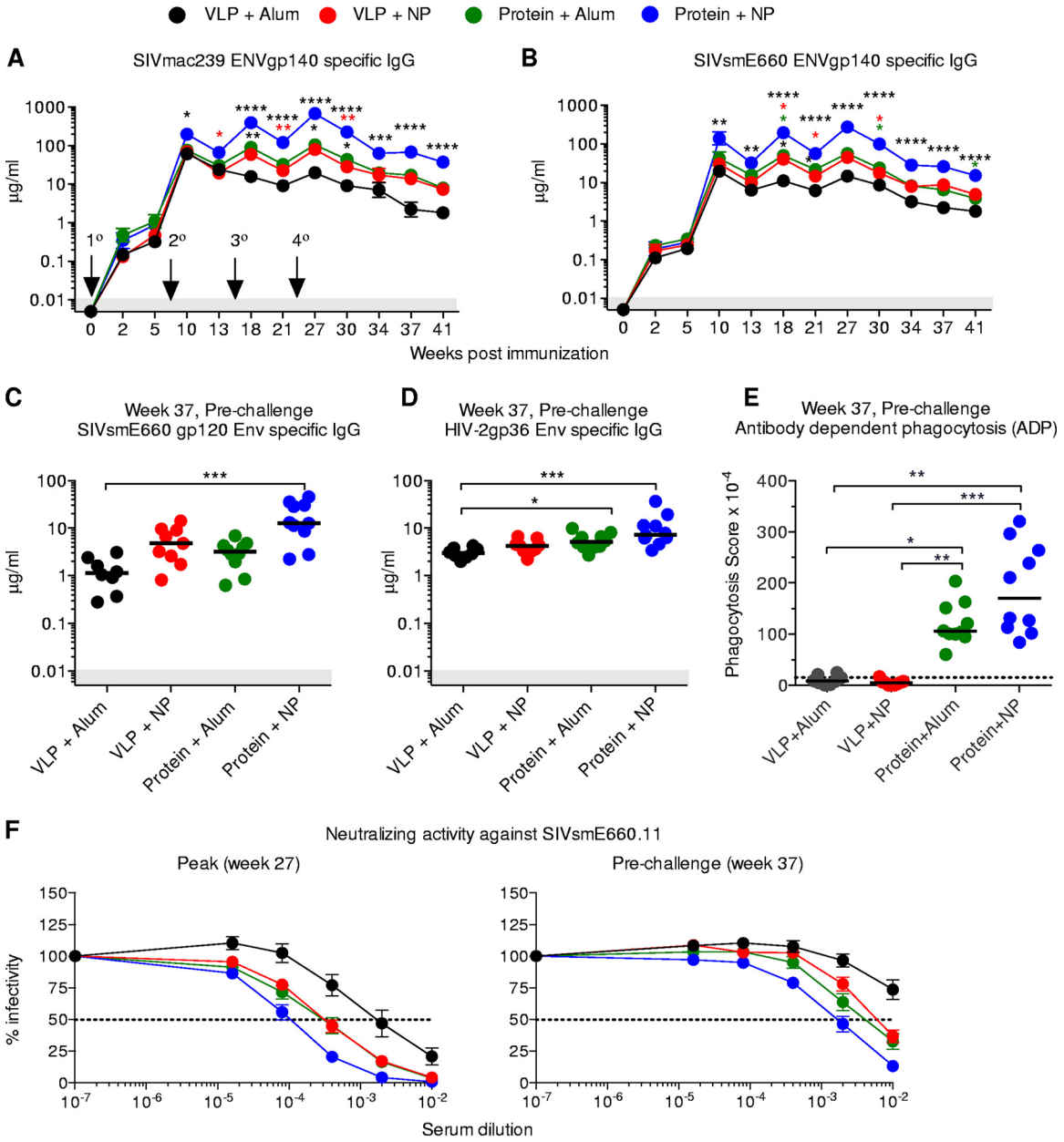

FIG 2 The NP adjuvant in the presence of the gp140 protein antigen significantly enhances systemic Env-specific humoral immune responses in RMs. (A and B) SIVmac239- and SIVsmE660-derived recombinant Env gp140-specific IgG binding antibody responses were assayed at the indicated time points. Binding titers are based on known standards, and the color-coded circles indicate the geometric mean ± standard error for ~8 to 10 animals per treatment groups. (C) SIVsmE660 Env gp120-specific binding responses were measured at week 37 (4 weeks prior to challenge). (D) HIV-2 gp36-specific binding responses were measured at week 37 (gp36 is an SIV gp41 homologue). (E) The ADP function associated with SIV Env-specific antibodies was measured at week 37. (F) SIVsmE660.11-specific neutralizing activity in serum was measured as week 27 (the time with the peak titer after the final immunization) and at week 37 (prechallenge). Serum dilution curves for each treatment group are shown. The graphs in panels C, D, and E are shown as scatter plots, with each dot representing an individual animal in the treatment groups and the horizontal lines indicating the median response. The statistical significance for differences between treatment groups in all graphs was evaluated using a multigroup comparison by the Kruskal-Wallis test followed by Dunn's correction. ****, $P < 0.0001$; ***, $P < 0.001$; **, $P < 0.01$; *, $P < 0.05$. Asterisks are placed above treatment groups for which the results are significantly different from those for the other approaches and are color coded to indicate the comparison between two respective groups.

NP adjuvant induces robust Env-specific plasmablast responses in blood and induces long-lived plasma cell responses in bone marrow and draining lymph nodes (LNs). The recall antibody response to vaccination in humans is characterized by a striking increase in antigen-specific plasmablasts in the peripheral blood at 7 days postvaccination (26). There is a relative paucity of data on the kinetics of the plasmab-

last response in macaques (27). Interestingly, immunized RMs exhibited significant Env-specific plasmablast responses at day 4 that contracted significantly by day 7 (Fig. 3A and B). The frequencies of IgG-secreting Env-specific plasmablasts were higher than those of IgA- or IgM-secreting Env-specific plasmablasts. Consistent with the Env-specific antibody responses, immunization with protein-NP induced significantly higher frequencies of Env-specific plasmablasts than the other immunization modalities (Fig. 3C and S3A). Env-specific plasmablast responses of comparable magnitudes were consistently detected after each booster immunization. As previously reported in humans (26), we observed a striking correlation between the frequencies of Env-specific early plasmablasts and the ensuing IgG binding antibody titers (data not shown).

The longevity of humoral responses has been attributed to the persistence of long-lived plasma cells (LLPCs) in the bone marrow (28). We assessed the frequencies of Env-specific plasma cells in the bone marrow after each booster immunization (Fig. 3D and S3B). The highest frequency of Env-specific LLPCs was found in animals immunized with protein-NP (Fig. 3D). Importantly, the frequency of LLPCs increased with every successive immunization. Four animals each immunized with protein-NP and protein-alum were sacrificed at 9 to 10 weeks after the final immunization (Fig. 1B) to analyze the B cell responses in various tissues. Strikingly, the frequencies of the LLPC responses were higher not only in the bone marrow but also in the draining iliac and popliteal lymph nodes of animals immunized with protein-NP than in animals immunized with protein-alum (Fig. 3E and F), a finding similar to what we had observed previously in mice (13). Of note, plasma cell responses remained restricted to draining lymphoid tissues upon repeated immunization at the same anatomical site, with negligible Env-specific plasma cells being observed in nondraining lymphoid tissues (Fig. 3F).

NP adjuvant induces higher Env-specific CD4$^+$ T cell responses than alum. We determined the frequencies of Env- and Gag-specific effector CD4$^+$ T cell responses in peripheral blood and lymphoid organs. Env-specific and cytokine (interferon [IFN] gamma [IFN-γ], tumor necrosis factor [TNF], or interleukin-2 [IL-2])-secreting CD4$^+$ T cell responses were found to be significantly higher upon immunization with protein-NP than upon immunization with the other immunization modalities after the final vaccination (Fig. S4A). These responses were also polyfunctional (i.e., they were capable of simultaneously eliciting the secretion of IFN-γ, TNF, and IL-2; Fig. S4B). Interestingly, the Env-specific responses elicited by VLPs were found to be polyfunctional after the primary immunization but less so after subsequent boosts. The Gag-specific responses were weaker than the Env-specific responses at each time point analyzed. Both Gag- and Env-specific CD8$^+$ T cell responses were observed to be very low or barely detectable across all animals in the study (data not shown). Before challenge, higher frequencies of follicular T helper (TFH) cells and GC B cells were observed in local draining (popliteal and iliac) LNs than in nondraining LNs (Fig. S5). These data show that immunization with protein-NP significantly enhances the Env-specific effector CD4$^+$ T cell responses in blood and at early time points induces TFH and GC cell responses in draining LNs comparable to those induced by alum.

NP-adjuvanted vaccines induce robust and persistent mucosal antibody responses. Antigen-specific antibodies at mucosal sites could offer protection against the mucosal transmission of HIV-1 (29). Accordingly, we evaluated the levels of the Env-specific IgG and IgA binding antibody responses in vaginal and rectal secretions at 2 weeks after each immunization and 1 month prior to challenge. Significantly higher Env-specific IgG and IgA responses were observed in the vaginal and rectal secretions of animals that received protein-NP both at 2 weeks after each immunization and at a prechallenge time point (4 weeks prior to challenge) (Fig. 4A to C). In contrast, Env-specific IgA responses in rectal secretions were only transiently elevated (Fig. 4D). A significant correlation between systemic and vaginal binding antibody (IgG and IgA) titers was observed in all immunized animals (Fig. 4E and F), suggesting a large

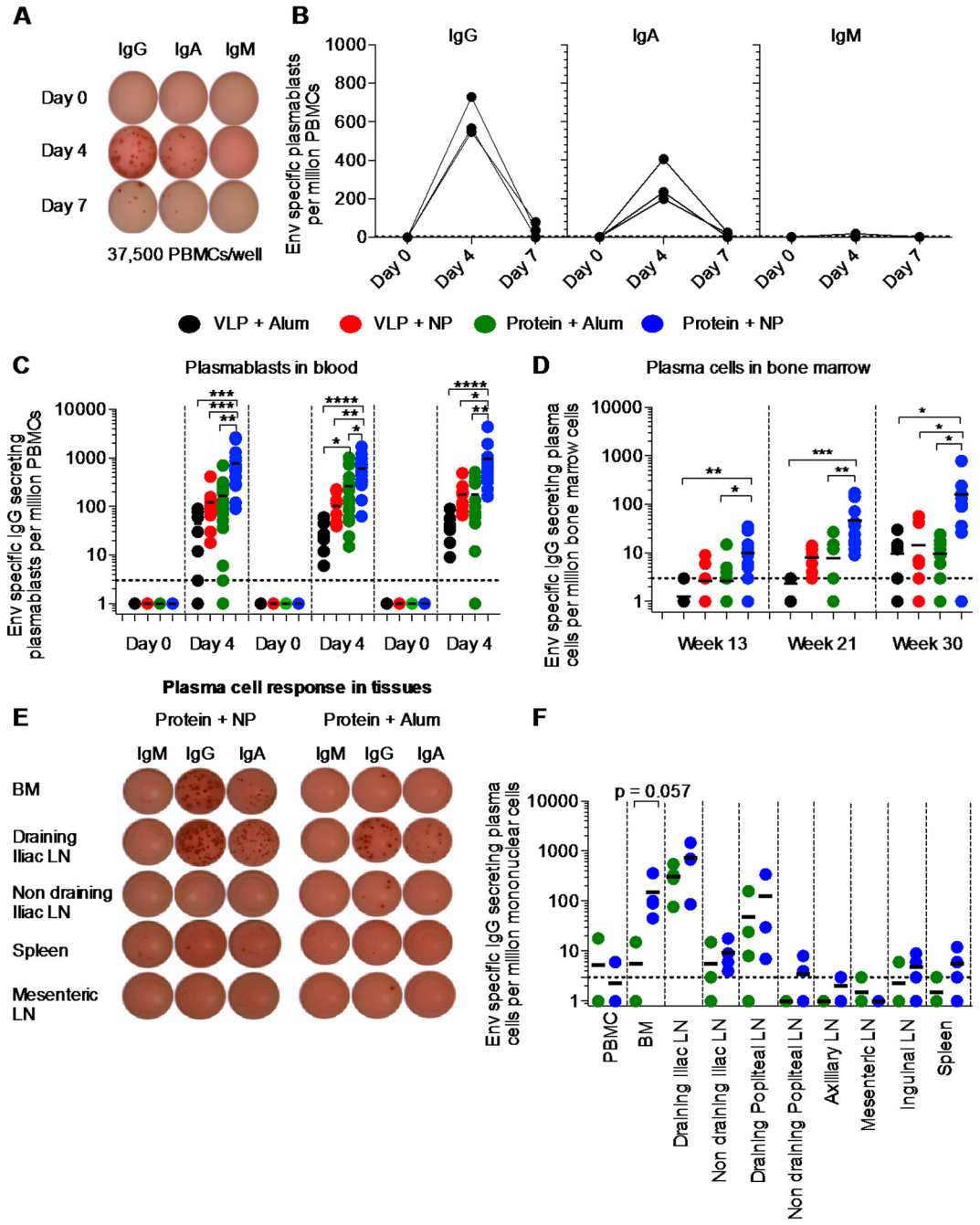

FIG 3 The NP adjuvant in the presence of the gp140 protein antigen significantly enhances Env-specific plasmablast responses in peripheral blood and persistent long-lived Env-specific plasma cells in bone marrow and draining lymph nodes in RMs. The frequency of Env-specific plasmablasts in peripheral blood and Env-specific plasma cells in the bone marrow and the secondary draining and nondraining lymphoid organs was determined by a B cell ELISPOT assay. (A) The peak plasmablast response in the peripheral blood of RMs was detected at day 4 after the boost immunizations. Env-specific IgG-, IgA-, and IgM-secreting B cells in wells from an ELISPOT assay plate for animals immunized with protein-NP at days 0, 4, and 7 after the first boost immunization in the study are shown. (B) Frequency of Env-specific IgG-, IgA-, and IgM-secreting plasmablasts per million PBMCs in one representative animal in the study. (C) Scatter plots of the magnitude of Env-specific IgG-secreting plasmablast responses at day 4 after each round of boost immunization in all treatment groups. (D) Scatter plots of the magnitude of Env-specific IgG-secreting plasma cells at 5 weeks following each round of boost immunization in all treatment groups. (E) Env-specific IgG-, IgA-, and IgM-secreting B cells in wells from an ELISPOT assay plate for one representative animal treated with protein-alum or NP adjuvant. (F) Frequencies of Env-specific IgG-secreting plasma cells per million total bone marrow cells in various draining and nondraining lymphoid organs at ~10 weeks after the final immunization. Horizontal bars, median responses. Statistical significance for the difference between treatment groups in panels C, D, and F was evaluated using a multigroup comparison by the Kruskal-Wallis test followed by the use of Dunn's correction. ****, $P < 0.0001$; ***, $P < 0.001$; **, $P < 0.01$; *, $P < 0.05$. BM, bone marrow.

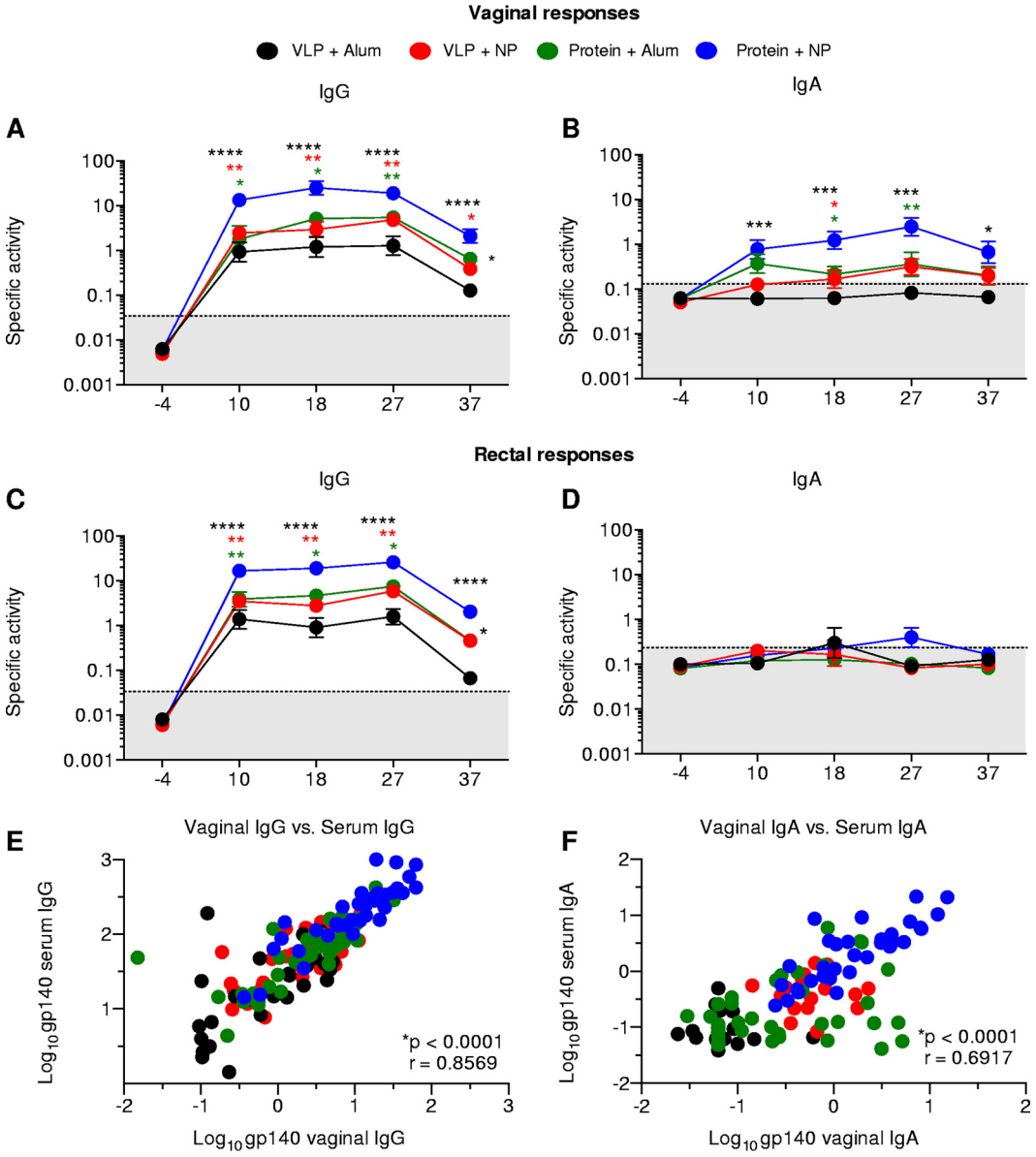

FIG 4 The NP adjuvant in the presence of the gp140 protein antigen significantly enhances the mucosal Env-specific humoral immune responses in RMs. Anti-SIV humoral responses in mucosal secretions postimmunization were measured by ELISA performed on vaginal and rectal secretions at the time of the peak titer after each immunization and at week 37 (4 weeks prior to challenge). (A and B) SIV Env-specific IgG and IgA titers in vaginal secretions, respectively. The titers reflect the Env-specific IgG or IgA concentration normalized to the total IgG or IgA concentration and is expressed as the number of nanograms of Env-specific IgG per microgram of total IgG. (C and D) SIV Env-specific IgG and IgA titers in rectal secretions. The circles on the line graph indicate the geometric mean ± standard error for ~8 to 10 animals per treatment group, as indicated in the legend to Fig. 1A. (E) Spearman's correlation of vaginal IgG responses at the time points indicated in panel A with the corresponding serum IgG responses. (F) Spearman's correlation of vaginal IgA responses at the time points indicated in panel B with the corresponding serum IgG responses. Spearman's *r* values and the *P* values of the correlations are indicated.

contribution of serum-derived antibodies in mucosal secretions. A similar correlation between the serum and rectal IgG binding antibody responses was observed (data not shown). Interestingly, the correlations for the IgA responses outlined above primarily relied on the responses from animals immunized with protein and not VLPs. Of note, local plasma cells were not detected in the vaginal or rectal tissues of animals in groups 3 and 4 after they were sacrificed (data not shown), further supporting the likelihood that mucosal antibodies are derived from serum.

NP-adjuvanted vaccines protect against vaginal acquisition of heterologous SIV in the presence of restrictive TRIM5α alleles. To test the efficacy of humoral

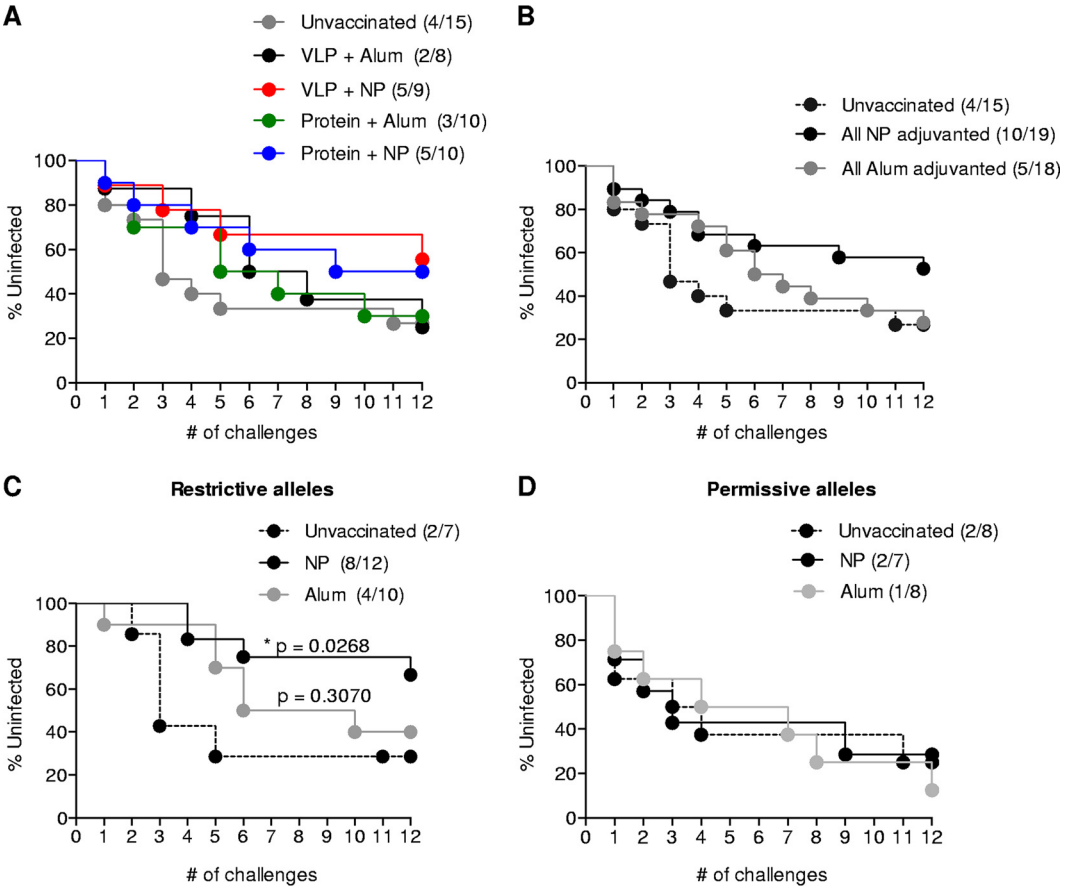

FIG 5 The NP adjuvant mediates enhanced protection against a low-dose intravaginal challenge with heterologous SIVsmE660 in the presence of restrictive TRIM5α in RMs. A Kaplan-Meier survival curve analysis was performed after a series of 12 weekly intravaginal challenges. (A) Survival curves for all treatment groups in the study, including unvaccinated control animals. The numbers in parentheses represent the number of uninfected animals at the end of 12 challenges/total number of animals. (B) Survival curves for all animals that received NP or alum adjuvant irrespective of antigen in comparison with the survival curve for unvaccinated control animals. (C) Survival curves for all animals bearing restrictive alleles that received NP or alum adjuvant. Survival curves were compared using a log-rank (Mantel-Cox) test, and a *P* value of <0.05 was considered significant.

immunity induced by vaccinations, the animals were intravaginally challenged with repeated exposures to low doses of a heterologous SIVsmE660 swarm (30–32). RMs were challenged once weekly for up to 12 exposures with SIVsmE660 (20,000 50% tissue culture infective doses [$TCID_{50}$] or 0.5 to 1 50% animal infective doses [AID_{50}]). The level of SIV RNA in plasma was monitored weekly, and an animal was considered infected if the viral loads were greater than 100 copies/ml in plasma for two consecutive weeks. The Kaplan-Meier curves shown in Fig. 5A depict the percentage of uninfected animals after each challenge. Approximately 50% of the unvaccinated naive animals were infected after four challenges, whereas six and seven challenges were required to infect 50% of the animals receiving protein-alum and VLP-alum, respectively. Ten challenges were required to infect 50% of the animals that received protein-NP, and even after 12 challenges, >50% of the animals receiving VLP-NP remained uninfected. However, statistical significance was not reached when the survival curves across treatment groups were compared with the survival curve for unvaccinated animals. To elucidate the role played by individual adjuvants (NP versus alum), we then combined the data for all animals by adjuvant irrespective of the form of antigen for survival analysis. Greater than 50% of all NP adjuvant-treated animals survived after 12 intravaginal viral challenges, whereas ~27% of unvaccinated or alum-treated survived animals ($P = 0.0786$, log-rank test, for NP-adjuvanted versus unvaccinated animals) (Fig. 5B). Since select TRIM5α alleles may confer partial resistance to the SIVsmE660 challenge strain, we included that parameter in the evaluation

(30, 32). Animals carrying either restrictive or permissive TRIM5α alleles were equally distributed in the treatment groups used in the study, as shown in Table S1. Mamu-A*001$^+$, Mamu-B*008$^-$, and Mamu-B*017$^-$ animals were also equally distributed among the treatment groups, even though these alleles have not previously been associated with resistance to the acquisition of the SIVsmE660 strain (30). The presence of restrictive TRIM5α alleles was not associated with protection in unvaccinated animals (Fig. 5C). However, the presence of the restrictive TRIM5α allele in animals immunized with the NP adjuvant appeared to significantly enhance resistance to the acquisition of virus ($P = 0.0286$, log-rank test). This observation did not translate to animals immunized with alum ($P = 0.3070$, log-rank test) when they were compared with unvaccinated animals. No protection was observed in animals carrying the permissive allele in the study (Fig. 5D). None of the vaccines appeared to significantly control viremia in the infected animals at either the peak (weeks 1 and 2) or the set point (week 12) (Fig. S6). These data suggest the ability of the NP adjuvant to enhance vaccine-mediated protection when it is combined with protein and VLP immunogens in the presence of restrictive antiviral alleles.

Serum and vaginal IgG responses correlate with protection in animals immunized with protein and NP adjuvant. The protective efficacy of 50% or greater observed in animals immunized with NP and either protein or VLP immunogens provided an opportunity to evaluate immune correlates. Env-specific serum IgG antibody responses in animals vaccinated with the protein-NP adjuvant were significantly higher ($P = 0.0317$, Mann-Whitney *t* test) in uninfected animals than infected animals at prechallenge time points of week 37 (Fig. 6A) and week 41 and on the day of challenge (data not shown). No such differences were observed in the other immunization groups. The SIVmac239 Env-specific IgG binding antibody responses in the vaginal secretions of animals immunized with protein-NP adjuvant were also significantly higher ($P = 0.0159$, Mann-Whitney test) in uninfected animals than infected animals (Fig. 6B). The antibody responses elicited by the protein-NP adjuvant showed a significant association with a delay in the acquisition of virus infection, as indicated by Spearman's correlation analysis, with the binding antibody responses to SIVmac239 Env, SIVsmE660 Env, and the SIV gp41 homologue HIV-2 gp36 and ADP activity (Fig. 6C to E). These associations held true irrespective of the presence of restrictive versus permissive TRIM5α alleles (Fig. 6C to F and S7). Similar associations were not observed in the other immunization groups (data not shown). Finally, the Env-specific CD4$^+$ T cell responses as well as the innate responses (the frequencies of monocyte and DC subsets), analyzed by flow cytometry at peak time points, also did not correlate with protection (data not shown).

NP and alum adjuvants mediate distinct innate immune responses. We have previously reported that different TLR agonists mediate distinct cellular and molecular signatures of early innate responses (33). Here, we compared the changes in the cellular and molecular signatures induced by NP and alum adjuvants. A significant expansion in the number of neutrophils in peripheral blood relative to that at the baseline was noted between 4 and 24 h postimmunization (Fig. S8A), while limited changes in the total number of peripheral blood mononuclear cells (PBMCs) were seen. However, among total PBMCs, a higher level of expansion of the number of lymphocytes was observed at days 7 and 14 in animals receiving the NP adjuvant than in those given alum (Fig. S8B). We developed a 12-color flow cytometry panel to evaluate the changes in the frequencies and the activation phenotypes of various individual cell types in peripheral blood at early time points postimmunization. We evaluated changes in monocyte subsets in RMs that included classical CD14$^+$ CD16$^-$ monocytes, intermediate CD14$^+$ CD16$^+$ monocytes, and nonclassical CD14$^{dim/-}$ CD16^{++} monocytes (Fig. 7A), as described before (11). The relative representation of CD14$^+$ CD16$^+$ monocytes was substantially increased after vaccination with NP adjuvants but not after vaccination with alum (Fig. 7B). Enhanced expression of CCR7, a chemokine receptor involved in homing to lymphoid organs, was observed on CD14$^+$ CD16$^-$ and CD14$^+$ CD16$^+$

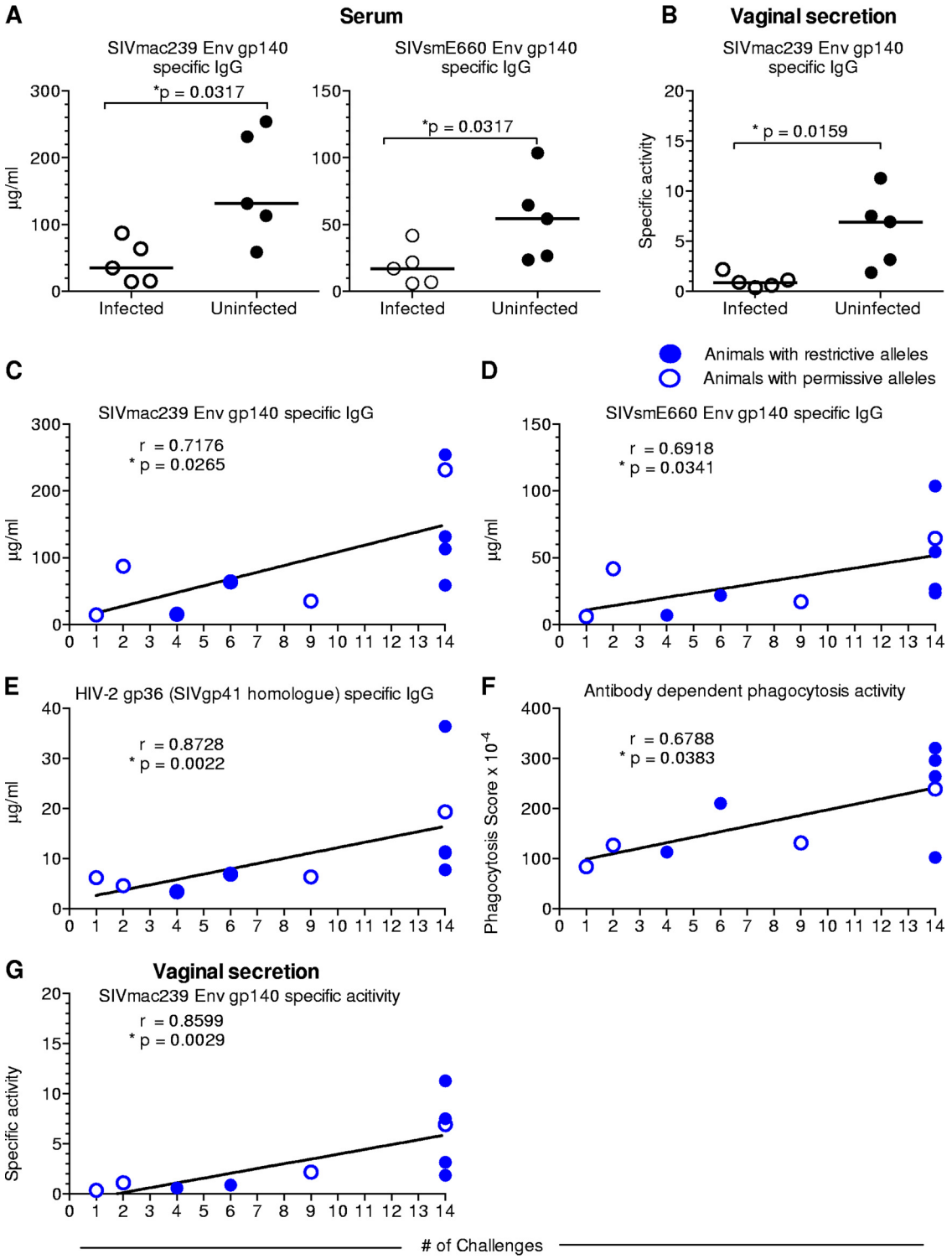

FIG 6 Binding antibody responses in serum and vaginal secretions in animals treated with protein-NP adjuvant significantly delay the onset of infection and correlate with protection. (A) SIVmac239 (left) and SIVsmE660 (right) Env-specific binding antibody response in the serum of infected and uninfected animals. *P* values were calculated using a Mann-Whitney rank sum test. (B) SIVmac239 Env-specific binding antibody response in vaginal secretions of infected and uninfected animals. (C and D) Correlation of the binding antibody responses (SIVmac239 and SIVsmE660 Env-specific IgG) with the ability to delay or prevent infection. (E and F) Correlation of the binding antibody responses (HIV-2 gp36-specific IgG and ADP activity) with the ability to delay or prevent infection. (G) Correlation of the binding antibody responses (SIVmac239 Env-specific IgG) in vaginal secretions with the ability to delay or prevent infection. Spearman's *r* values and the associated *P* values of significance are listed. *P* values were not adjusted for multiple comparisons.

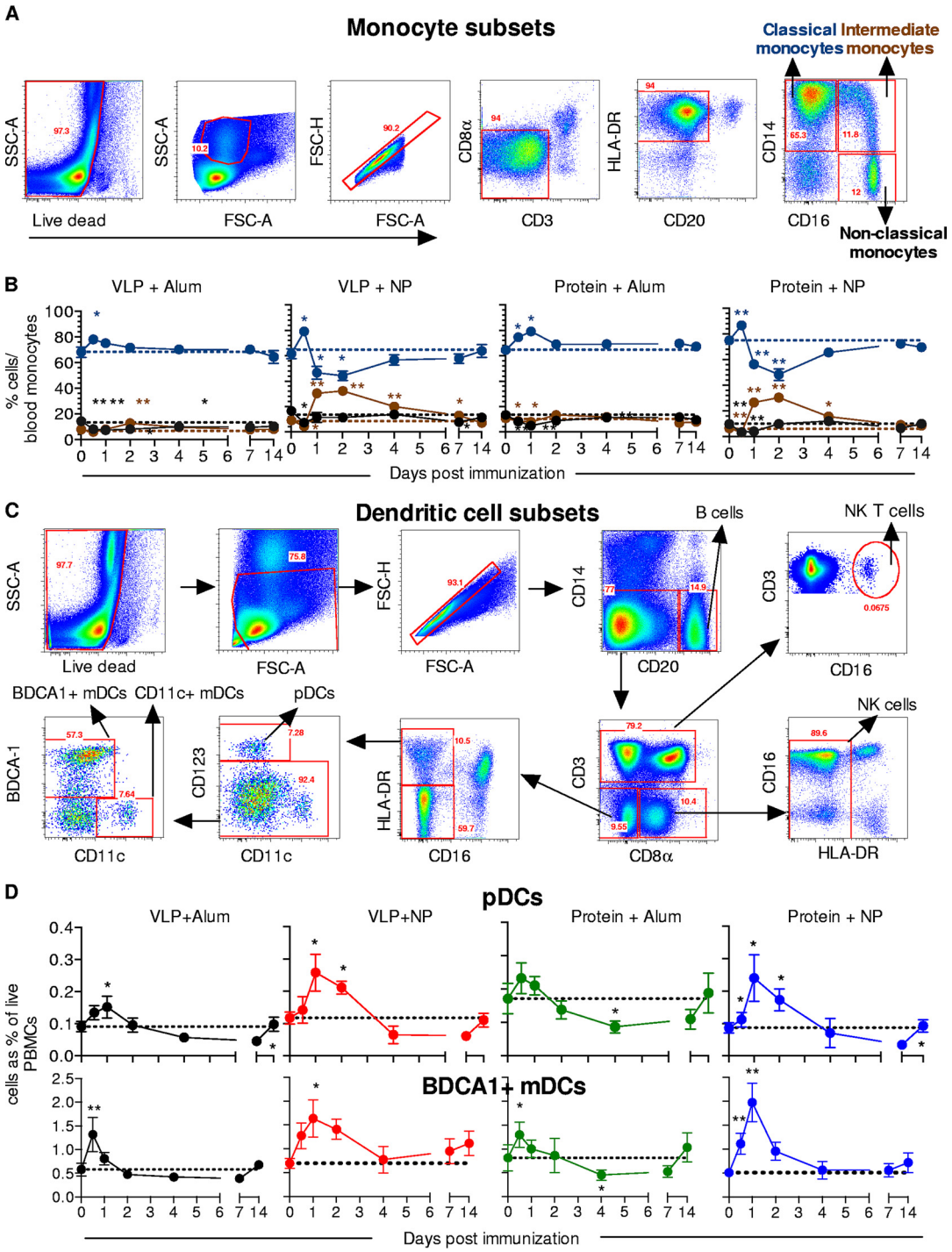

FIG 7 NP and alum adjuvants stimulate distinct early innate responses. The changes in cell frequency and activation induced by both adjuvants were measured using flow cytometry. (A) The flow cytometry gating strategy used to identify monocyte subsets, namely, the CD14$^+$ CD16$^-$ classical monocytes, CD14$^+$ CD16$^+$ intermediate monocytes, and CD14$^-$ CD16^{++} nonclassical subsets, is shown. Numbers in the flow cytometry plots (A and C) refer to cell frequencies that appear within the gate drawn to specify cell events. (B) Changes in monocyte subsets as a fraction of the total monocytes in peripheral blood after primary immunization. Blue lines, classical monocytes; brown lines, inflammatory monocytes; black lines, nonclassical monocytes. (C) The flow cytometry gating strategy used to identify changes in cell populations in peripheral blood is highlighted. pDCs were identified as CD14$^-$ CD20$^-$ CD3$^-$ CD8α^- CD16$^-$ HLADR$^+$ CD11c$^-$ CD123$^+$ cells. Two subsets of mDCs are highlighted: BDCA-1 mDCs (CD14$^-$ CD20$^-$ CD3$^-$ CD8α^- CD16$^-$ HLADR$^+$ CD123$^-$ CD11c$^{lo/-}$ CD1c$^+$ cells) and CD11c$^+$ mDCs (CD14$^-$ CD20$^-$ CD3$^-$ CD8α^- CD16$^-$ HLADR$^+$ CD123$^-$ CD1c$^-$ CD11c$^+$ cells). (D) Changes in pDC, mDC1, and mDC2 subsets in peripheral blood after primary immunization. Dotted lines, mean baseline frequencies of cell subsets in animals allocated to each treatment group. The statistical significance of the change in the frequencies of cell subsets in comparison with those at the baseline was determined using a paired nonparametric Wilcoxon matched-pairs signed-rank test. **, $P < 0.01$; *, $P < 0.05$. SSC, side scatter; FSC, forward scatter.

monocytes upon immunization with alum or NP adjuvants (Fig. S9). Minimal changes in the expression level of CCR7 on CD14$^{dim/-}$ CD16^{++} monocytes were observed. In contrast, CD14$^{dim/-}$ CD16^{++} monocytes had more prominent changes with CD86 expression at day 2 and day 4 in all animals except those immunized with protein and alum, though the change was most evident in animals immunized with protein-NP (Fig. S10). Only modest changes in CD86 expression on classical and intermediate monocytes were noted. The identification of various cell types in peripheral blood is detailed in the flow cytometry gating scheme shown in Fig. 7C. A significant expansion of the plasmacytoid DC (pDC) and myeloid DC (mDC) subsets with BDCA-1^{+} CD11c$^{lo/neg}$ cells was observed, with elevated numbers of mDCs persisting longer in NP-immunized animals than alum-immunized animals (Fig. 7D). Minimal change in CD11c^{hi} BDCA-1^{lo} mDCs was observed (data not shown). The increased expression of CCR7 on all DC subsets (Fig. S11) and of CD86 only on mDC subsets (Fig. S12) was higher and more persistent when animals were immunized with the NP adjuvant than when they were immunized with alum. A significant decrease in the frequency of B cells in peripheral blood was observed in animals immunized with protein-NP, suggesting recruitment to lymphoid organs (Fig. S13). In contrast, a limited change in the frequencies of T cells, NK cells, and NK T cells was observed across all groups (Fig. S13).

Blood transcriptional signatures that correlate with Env-specific antibody titers in vaginal secretions and protection against infection. We next assessed the transcriptome changes in the PBMCs of animals immunized with the NP or alum adjuvant. Unsupervised principal component analysis (PCA) revealed that animals immunized with NP have a distinct gene expression profile at 24 h to 96 h postimmunization compared to the profile for animals immunized with alum (Fig. 8A). The NP adjuvant appeared to induce a larger transcriptional response than alum (Fig. 8B), as many genes were uniquely induced in groups immunized with the NP adjuvant (Fig. 8C, orange bars). Additionally, most of the genes which were differentially expressed in the alum-treated groups were also differentially expressed in the NP-treated groups (Fig. 8C, pink bars), suggesting that alum and NP may share an overlapping molecular mechanism of action during the initial hours postimmunization (Table S2).

We hypothesized that the TLR ligands in our NP formulation would trigger genes similar to those induced by the YF-17D vaccine (34). The levels of expression of several type I interferon and antiviral genes were found to be similar to the levels of expression of such genes induced by the YF-17D vaccine in humans (34) and were observed to be persistently higher in animals that received the NP adjuvant than in those immunized with alum (Fig. 8D). This suggests that the NP adjuvant induces a transcriptional program that is similar to that induced by live attenuated viruses.

One of the key findings of this study is the identification of an immunological correlate of protection; that is, in animals vaccinated with the NP adjuvant plus protein, the magnitude of the binding antigen-specific IgG response in the serum and in vaginal secretions on the day of challenge is correlated with protection against infection (Fig. 6). We wished to determine whether there were transcriptional signatures in the blood, induced within hours or days after vaccination, which correlated with protection and/or the immunological correlate. Thus, we analyzed gene signatures that were correlated with immunogenicity (vaginal IgG titers) and with protection in animals immunized with protein-NP (Fig. 9A). Although some genes were associated only with vaginal IgG titers (Fig. 9B, orange bars), hundreds of other genes were associated with both immunogenicity and protection outcome (Fig. 9B, purple bars, and Table S2). We next performed gene set enrichment analysis (GSEA) (35) of genes ranked by their correlation scores and by using blood transcription modules (BTMs) (36) as gene sets (Table S2). This analysis revealed that 4 different NK cell modules and 3 different T cell-related BTMs were positively correlated with protection as well as with vaginal antibody titers (Fig. 9C). Interestingly, this positive correlation was observed throughout the first several days, suggesting an ongoing role for NK cells and T cells in promoting antibody-mediated protection against infection. Furthermore, innate antiviral and type I IFN modules were positively correlated with protection against infection and vaginal

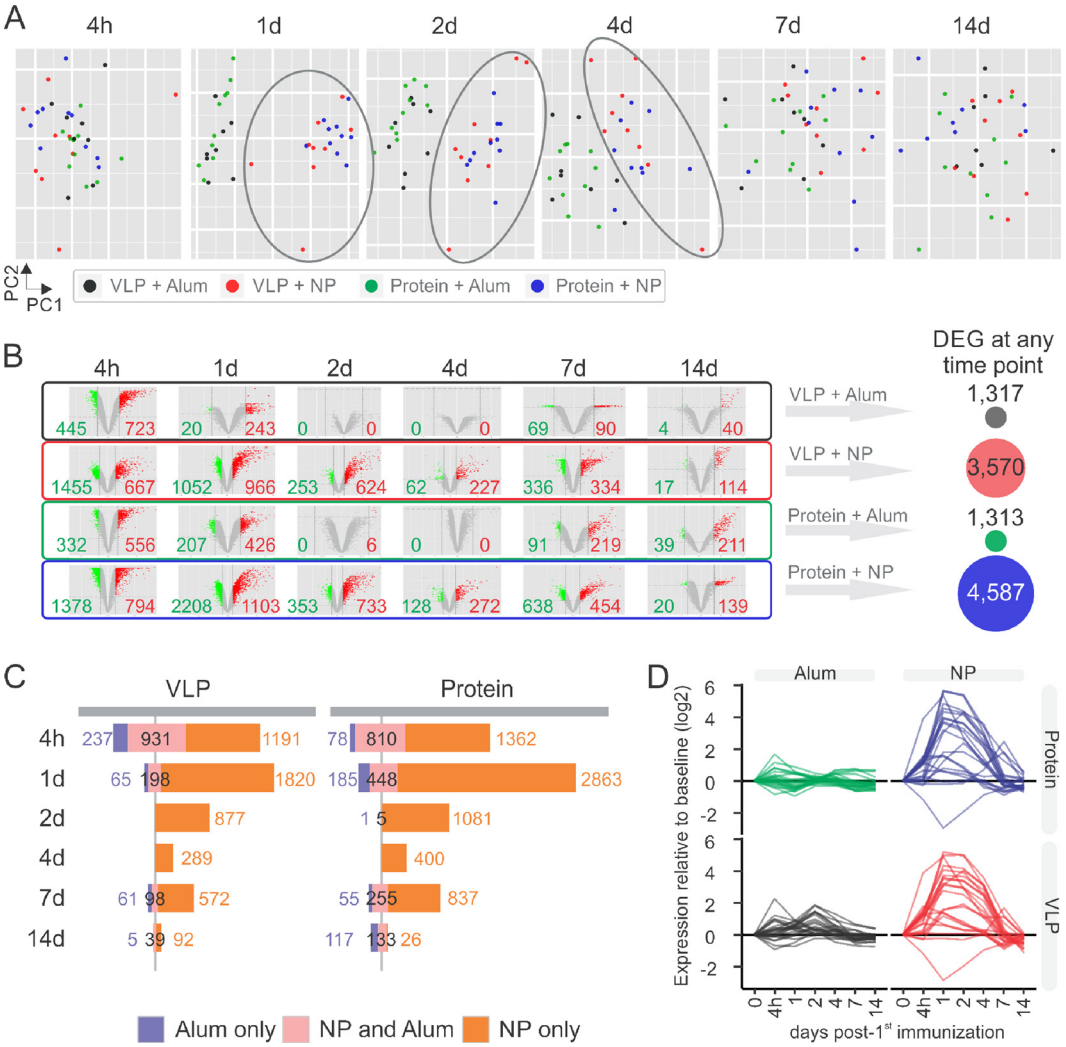

FIG 8 NP and alum adjuvants induce early changes in the transcriptome in blood. The gene expression profiles in the blood of animals during the initial 14 days after primary immunization are shown. (A) Principal component analysis was performed for each time point using the 5,000 most variable genes (see Materials and Methods). Gray ovals, samples from animals that received the NP adjuvant. (B) Differentially expressed genes (DEG) per time point and per group of treatment. (C) Number of differentially expressed genes unique (purple and orange bars) or in common (pink bars) to NP and alum groups. (D) Temporal expression pattern of genes from blood transcription module M75 (antiviral IFN signature) in each treatment group.

IgG titers, but only during the first 4 h (Fig. 9C). In addition, there was a striking but transient (only at 48 h) association between at least 4 BTMs related to monocytes, TLRs, and inflammatory signaling and neutrophils and both protection and vaginal IgG titers on the day of challenge. This transient association is consistent with the transient change in the relative representations of $CD14^+$ $CD16^-$ classical monocytes versus $CD14^+$ $CD16^+$ inflammatory monocytes, which was most striking at 2 days after vaccination (Fig. 7B), and may reflect the migration of specific subsets of monocytes from the blood to the lymphoid organs, where they may promote antibody responses (33). Taken together, these results demonstrate that the transcriptional signatures found to be induced in the blood within a few hours of vaccination with NP plus protein represent an early molecular correlate of immunogenicity and protection.

Finally, given our inability to identify any immunologic correlate of protection for animals immunized with VLP-NP, we wished to determine whether there were early transcriptional signatures that correlated with protection in animals immunized with VLP-NP. Our analysis revealed that, similar to the case in animals immunized with protein-NP, BTMs related to NK cells and T cells were positively correlated with protection (Fig. 9C).

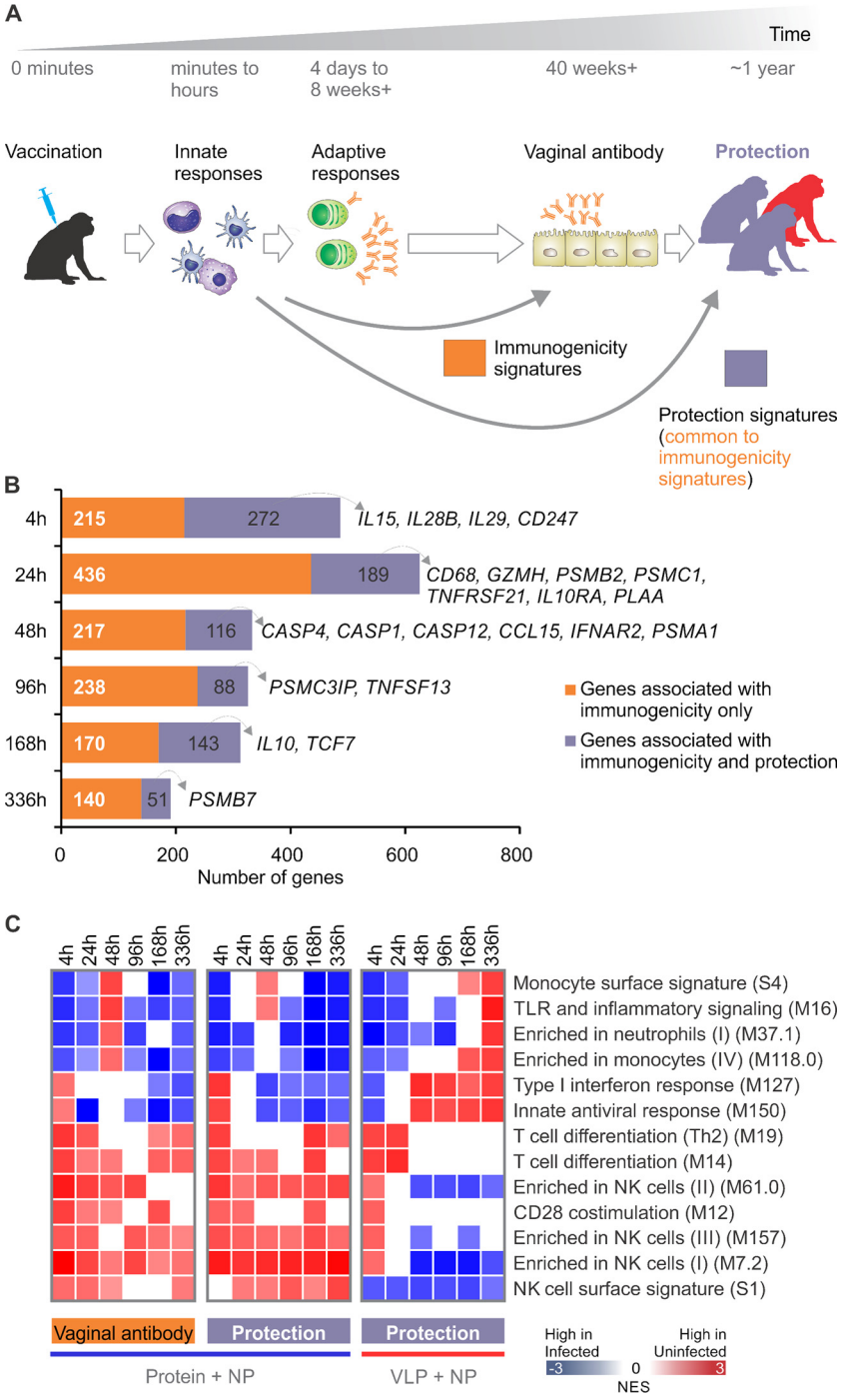

FIG 9 Signatures of immunogenicity and protection. (A) We compared the baseline-normalized expression data from the initial 14 days after primary immunization with the vaginal antibody responses (signatures of immunogenicity) and protection outcomes (signatures of protection), which were defined after 40 weeks and almost 1 year after the primary immunization, respectively. (B) Genes whose baseline-normalized expression data were correlated with prechallenge vaginal SIVmac239 Env-specific IgG antibody titers ($P < 0.01$) and/or were different between infected and uninfected animals postchallenge (adjusted P value, <0.05; mean fold change, >1.25). Orange bars, genes found only in the signatures of immunogenicity; purple bars, genes found in both signatures. Selected genes are indicated by gray arrowheads. (C) BTMs associated with protection outcome and identified by GSEA (nominal P value, <0.05). Colors represent higher levels of expression in infected (blue) or uninfected (red) animals, with the lighter and darker shades of the two colors indicating lower and higher levels of expression, respectively.

However, unlike the case with protein-NP, this association was transient and observed only at 4 to 24 h. Furthermore, similar to the results obtained with the protein-NP group, there was a positive correlation between the expression of BTMs representing antiviral and type I IFN genes and protection, but this was observed only between 48 h and 14 days (Fig. 9C).

DISCUSSION

Our previous work has described the synthesis of poly(lactic-co-glycolic) acid (PLGA)-based NP-encapsulated TLR ligands and demonstrated their efficacy as vaccine adjuvants in mice (13). This work demonstrated the superior ability of such adjuvants to stimulate antigen-specific B and T cell responses compared with that of alum, which is the adjuvant most widely used today. A key question raised by our previous work was whether these NP-based adjuvants would demonstrate superior immunogenicity in nonhuman primates. In the current study, we have demonstrated that NP-encapsulated TLR ligands induce robust and persistent antibody responses against SIVmac239 Env immunogens in RMs. A key goal of this study was to compare the immunogenicity of the soluble gp140 Env protein immunogen with that of Env expressed on the surface of VLPs. Gag-Env pseudoviruses bearing native HIV Env trimers have been well characterized (19). The data in Fig. 2 demonstrate a greater magnitude of Env-specific antibody responses in animals vaccinated with soluble gp140 protein than in those vaccinated with VLPs. A caveat to this interpretation is that the ELISA used to measure Env-specific antibodies used the soluble gp140 protein and, hence, may have biased the results toward the detection of antibodies elicited by this form of the immunogen. While this is formally possible, it appears to be unlikely, since an alternative ELISA using concanavalin A-captured VLP Env yielded the same result (data not shown). Furthermore, serum from protein-immunized animals had greater neutralizing activity in assays dependent on live pseudovirus with native Env (Fig. 2F). Based on these data, we conclude that soluble gp140 immunogens are more immunogenic than VLPs when administered with the NP adjuvant. Finally, when the NP adjuvant was used with the soluble gp140 immunogen, it was also successful in mediating an Env-specific IgG response of a substantially larger magnitude than the IgA responses in serum (Fig. 1 and S1). Given that Env-specific IgA was reported to correlate negatively with protection, presumably by competing with Env-specific IgG (5), the ratio of IgG/IgA could have played a critical role in the protection observed in the current study.

The enhanced magnitude of Env-specific antibody responses was mirrored by a robust plasmablast response in the blood. Vaccination using either alum or NP adjuvant demonstrated that plasmablast responses in RMs appear rapidly (day 4) (Fig. 3) and earlier than previously reported in both RMs (37) and humans (26). Variable contraction of the immune response by day 7 has been observed in follow-up studies, depending on the nature, dose of immunogen, and adjuvant (unpublished data). Of note, greater than 75 to 80% of the plasmablast responses were Env specific (27). A striking finding was that NP adjuvants were also capable of inducing long-lived plasma cell responses in the bone marrow as well as in the draining Iliac and popliteal LNs that persisted for several months after vaccination. This is consistent with the findings of our previous studies in mice, where NP adjuvant induced robust antibody responses and persistent germinal center and plasma cell responses in the draining LNs (13). Also, in additional experiments with an HIV-1-derived Env immunogen with NP encapsulating a novel TLR7/8 ligand with a fatty acid tail (which likely results in enhanced persistence of the adjuvant), the magnitude and durability (up to 1 year) of the Env-specific immune responses in macaques were significantly enhanced in comparison with those achieved with alum (unpublished data).

In other vaccine studies with nonhuman primates, the induction of mucosal IgA responses at sites of subsequent viral exposure has been associated with sterile protection, delayed acquisition of infection, or improved control of SIV or simian-human immunodeficiency virus (SHIV) infection (38–42). However, it is clear from passive immunization studies that IgG neutralizing antibodies in serum can also prevent rectal or vaginal transmission of SHIV in macaques (43–45). Some nonneutral-

izing IgG monoclonal antibodies, especially those to the gp41 immunodominant region, have also been found to confer resistance or reduce the number of transmitted/founder variants in vaginally challenged RMs (43, 46, 47). In this study, there was a striking induction and persistence of Env-specific IgG and IgA in both the serum and vaginal secretions of animals immunized with protein-NP. The anti-Env antibodies in vaginal secretions were concluded to have originated from serum because the levels were highly correlated (Fig. 4E and F), and no Env-specific antibody-secreting cells (ASCs) were detected in vaginal tissue (data not shown). As the levels of anti-Env IgG but not those of anti-Env IgA in these secretions were associated with protection, our data suggest that nonneutralizing serum IgG (but not IgA) that transudates into vaginal tissues and secretions may play a significant role in preventing vaginal virus transmission. On the other hand, we postulate that even greater protection might perhaps be achieved if both mucosal IgA and serum IgG antibody responses can be induced (48).

The protective efficacy of the NP-adjuvanted vaccines was assessed by repeated low-dose intravaginal challenge with the heterologous strain SIVsmE660. There was enhanced protection in animals that received the NP adjuvant relative to those that received alum (Fig. 5), which was most apparent in animals with TRIM5α restrictive alleles. Interestingly, the degree of protection was similar in animals that were immunized with either the protein or the VLP immunogen (Fig. 5). In such animals, protection was induced by immunization with NP adjuvants (but not with alum). This suggests a synergy between host restriction factors and vaccine-induced immune responses in mediating protection against SIV infection (32). The mechanistic basis of why such a synergy was observed only in animals receiving the NP adjuvant and not alum is unclear. One possible explanation, proposed by Letvin et al. (32), suggests that the higher levels of prechallenge serum (Fig. 1) and vaginal (Fig. 4) IgG in NP-adjuvanted animals could bind to SIV virions and decrease the effective inoculum available to infect the animal. As a consequence, the lowered residual load of infectious virions is susceptible to TRIM5α-mediated restriction. A role for type I IFN in the induction of innate restriction factors, such as TRIM5α, APOBEC3, and tetherin, is well documented (49). As such, a strong type I IFN response induced by the NP adjuvant (Fig. 8D) may have also partially contributed to protection. However, while the type I IFN-based antiviral responses stimulated by the NP adjuvant were higher and more persistent in peripheral blood than those stimulated by alum, it is unclear if the level of expression of innate host restriction factors in local (vaginal and rectal) tissues was also elevated. Future work should be aimed at systematically assessing this. Finally, a closer look at the innate restriction factors induced by adjuvants in human clinical trials may also yield additional insight into the development of adjuvants for HIV vaccines.

Partial or significant protection against a heterologous challenge with neutralization-sensitive or -resistant SIV variants as well as SIV/HIV chimeric challenge in vaccinated animals in comparison with that in unvaccinated controls has been demonstrated in RMs. Vaccine approaches in many of these studies included priming with plasmid DNA encoding SIV/HIV immunogens followed by the administration of viral vectors (modified vaccinia virus Ankara, adenovirus type 5) (31, 32, 50) or priming with viral vectors followed by recombinant protein boosts (39, 51–55). Consistent with the findings of these studies, analysis of correlates of protection in our current study revealed that the magnitude of the Env-specific binding antibody titers at week 37 prechallenge correlated strongly with the protection induced by immunization with protein-NP (Fig. 6). In contrast, no positive trends between antibody responses and protection outcome were observed in animals immunized with VLP-NP (data not shown). A modest yet significant association with increased acquisition of challenge virus was observed when correlating with the anti- SIVmac239-derived Env-specific binding antibody response (data not shown).

Flow cytometry- and systems-based approaches demonstrate that the innate immune responses and transcriptional signatures induced by NP adjuvants are very distinct from those induced by alum. We recently highlighted differences in the innate immune responses in peripheral blood and draining LNs induced by ligands for TLRs 4,

7/8, and 9 in nonhuman primates (33). A TLR7/8 ligand (R848) induced the mobilization, activation, and expansion of $CD14^{+}$ $CD16^{++}$ intermediate monocytes both in peripheral blood and in draining LNs. More recently, we have also demonstrated that $CD14^{+}$ $CD16^{++}$ intermediate monocytes infected with dengue virus (DENV) help with the differentiation of resting B cells into plasmablasts and enhanced immunoglobulin (IgG and IgM) production via the B cell-activating factor (BAFF), A proliferation-inducing ligand (APRIL), and IL-10 cytokines (56). Consistent with these observations, in our current study, the NP adjuvant led to the significant expansion of $CD14^{+}$ $CD16^{++}$ intermediate monocytes in peripheral blood at days 1 and 2 postvaccination in comparison with the findings for the alum adjuvant, where no such expansion was seen (Fig. 7B). Our data suggest that intermediate monocytes mobilized by the NP adjuvant could have contributed to the significantly higher level of expansion of Env-specific plasmablasts in peripheral blood and long-lived plasma cells in bone marrow in comparison with that achieved with alum (Fig. 3). Furthermore, the NP adjuvant was more potent than alum in its ability to activate monocyte subsets (Fig. S9 and S10) and DC subsets (Fig. S12 and S13).

Finally, NP adjuvants induced an antiviral type I IFN signature with temporal patterns similar to those induced by the live attenuated yellow fever vaccine (34). This analysis also revealed transcriptional signatures that correlate with both the immunogenicity (antigen-specific antibody titers in vaginal secretions on the day of challenge) and the protection induced by vaccination with protein-NP. The identification of early blood transcriptional signatures that correlate with the ensuing Env-specific antibody titers in vaginal secretions and protection against infection addresses an important problem in vaccinology, that is, how to identify blood biomarkers for mucosal immunity and protection against mucosal infection. However, the robustness of these signatures in their ability to predict protective immunity remains to be tested in an independent cohort of animals in future studies. Taken together, these results demonstrate that NP-encapsulated TLR ligands promote robust and durable antibody responses in RMs that contribute to protection against mucosal challenge and reveal hitherto unappreciated mechanisms by which such adjuvants drive the innate and adaptive response to vaccination.

MATERIALS AND METHODS

Soluble Env and Gag immunogens. Recombinant SIVmac239-derived Env gp140 protein purified from an HEK293 cell culture was procured from Immune Technology Corp., New York, NY, USA. The endotoxin level was certified to be <50 endotoxin units (EU)/mg (equivalent to <2.5 EU/dose in the study). Recombinant p55 Gag protein produced in insect cells was procured from Protein Sciences Corporation, Meriden, CT, USA. Protein was certified to have endotoxin levels of <10 EU/mg (<1 EU/dose in the study).

Generation of SIVmac239 VLP-producing 293F cell lines. 293F cells were transfected with pCDNA4/TO (Life Technologies) expressing SIVmac239 Gag. Stable transfectants were selected in zeocin (Life Technologies), and clonal populations were derived by limiting dilution. Following doxycycline induction, the levels of cellular and supernatant Gag and Env expression were established by Western blotting. Clones generating high yields of Gag-Env particles with complete cleavage of Env were selected for further use as a Gag VLP-producing cell line. This line was transfected with SIVmac239 Env in the vector pCDNA5/TO-puro (Life Technologies), and selection under puromycin was performed. Subsequent Gag and Env expression clones were derived as described above. SIV Gag-Env VLPs were harvested after 48 to 72 h of doxycycline induction for further characterization. VLPs were analyzed on 20 to 60% sucrose gradients, with fractions being harvested and concentrated for analysis by Western blotting. Cells expressing Gag-Env VLPs were fixed and prepared for transmission electron microscopy as previously described (18). Images were acquired on a Hitachi H-7500 transmission electron microscope.

Procedures for purification of large-scale SIV VLP batches. SIV Gag-Env-producing 293F cells were grown in 5-liter spinner flasks and induced with doxycycline for 48 to 72 h. Supernatants were harvested, filtered through 0.45-μm-pore-size filters, and purified and concentrated by cross-flow (tangential) filtration using hollow-fiber cartridges and phosphate-buffered saline as the buffer.

Adjuvants. Alum (aluminum hydroxide; 2%; Alhydrogel) adjuvant was procured from InvivoGen. The alum dose was fixed at a 500-μg equivalent aluminum content as previously established in human studies (21, 22). Purified monophosphoryl lipid A (MPL) was procured from Avanti Lipids, AL, USA. The TLR7/8 agonist R848 was procured from Enzo Life Sciences. Poly(lactic-co-glycolic) acid (PLGA) was procured from Boehringer Ingelheim. Poly(vinyl alcohol) (PVA) was procured from Sigma-Aldrich. PLGA nanoparticles containing MPL and R848 were synthesized using an oil-in-water single emulsion followed by a solvent evaporation process as described before (13) with slight modifications. Briefly, the organic

phase containing PLGA with MPL and R848 was homogenized with 15 ml of a 5% (wt/vol) solution of PVA for 2 min using a Powergen homogenizer (Fisher Scientific) at a speed setting of 6. The oil-in-water emulsion was then solvent evaporated for 4 h at room temperature in a total volume of 100 ml. The nanoparticles that formed were collected by centrifugation and washed with 50 ml of 0.2-μm-pore-size filter-sterilized deionized water 2 times. The nanoparticle suspension was snap-frozen in liquid nitrogen and lyophilized using a FreeZone 2.5-liter benchtop lyophilizer (Labconco). Twenty milligrams of nanoparticles containing 50 μg of MPL and 750 μg of R848 was used in all NP immunizations.

Animals. Seventy-two female Indian RMs were used in the study. The animals were confirmed to be negative for SIV and simian T cell lymphotropic virus (STLV). The age range of the animals used in the study was 5 to 19 years. Animals were equally distributed among the treatment approaches on the basis of age and expression of the Mamu-A*001$^+$, Mamu-B*008$^+$, and Mamu-B*017$^+$ alleles. TRIM5α genotyping was conducted as previously described (57), and restrictive (high) or permissive (moderate) alleles were also equally distributed among the groups. All animal procedures were performed in accordance with guidelines established by the Emory University School of Medicine Institutional Animal Care and Use Committee. Ten animals were assigned to each immunization group and used in challenge studies after four rounds of immunization. Two animals receiving treatment with VLP and alum and one animal given VLP and NP were withdrawn from the study for clinical reasons unrelated to the study. An additional 16 animals were allocated to groups receiving protein-alum and protein-NP, where 4 animals from each treatment group were sacrificed after each round of immunization to investigate organ-specific immune responses.

Immunization and sampling. Animals were immunized 4 times with ~8-week intervals between each round of immunization. Subcutaneous immunizations were carried out in the lower limb at a location behind the knee close to the popliteal LN. For VLP immunizations with alum, VLPs containing 50 μg of Env and 1.5 mg Gag were gently mixed with 500 μg of alum at room temperature. The mixture was maintained on ice until it was used for the immunizations, and the animals were immunized with a final volume of 1.2 ml. For VLP immunizations with NP adjuvant, NPs containing 50 μg of MPL and 750 μg of R848 were suspended in PBS. The mixture was briefly sonicated, vortexed, and mixed with VLPs before gentle mixing with VLPs using low-speed vortexing. Animals were immunized with a final volume of 1.2 ml. For immunizations with protein and adjuvants, recombinant Env and Gag proteins were diluted in PBS and mixed with the alum or NP adjuvant as described above, and the final doses were 50 μg of Env and 50 μg of Gag. All immunizations and blood and mucosal tissue samplings were performed while the animals were under sedation, induced with 10 mg/kg of body weight ketamine. The animals were weighed each time that they were accessed for sampling.

Challenge stock of virus and intravaginal challenge. The RMs underwent a total of up to 12 challenges with SIVsmE660 (courtesy of Nancy Miller, NIAID), delivered intravaginally in a volume of 1 ml once a week. Each challenge dose contained virus at 2×10^4 $TCID_{50}$ and was titrated to represent an AID_{50} of ~0.5 to 1. The virus stock was grown in pigtailed macaque primary cell cultures.

Analysis of anti-Env and anti-Gag plasmablast responses in blood and plasma cell responses in bone marrow. Enzyme-linked immunosorbent spot (ELISPOT) assays were performed as previously described (26, 58), with some modifications. Briefly, 96-well multiscreen HTS filter plates (catalog number MSHAN4B50; Millipore) were coated overnight at 4°C with 10 μg/ml of anti-monkey IgG, IgA, or IgM (H&L) goat antibody (Rockland) or with 2 μg/ml of recombinant SIV gp140 or Gag protein (Immune Technology Corp.) for enumeration of total or antigen-specific antibody-secreting cells (ASCs), respectively. The wells were washed 4 times with PBS–0.05% Tween 20 (PBS-T) and 4 times with PBS and blocked with complete RPMI 1640 medium (supplemented with 10% fetal bovine serum [FBS] and penicillin-streptomycin) for 2 h in a 5% CO_2 incubator at 37°C. Whole PBMC preparations or PBMC-derived sorted cells were diluted in complete RPMI 1640 medium, plated in serial 3-fold dilutions, and incubated overnight in a 5% CO_2 incubator at 37°C. The wells were washed 4 times with PBS and 4 times with PBS-T, followed by incubation with either anti-monkey IgG-, IgA-, or IgM-biotin-conjugated antibodies (Rockland), and diluted 1:1,000 in PBS–0.05% Tween 20–1% FBS solution (PBS-T-F) for 2 h at room temperature. The wells were again washed 4 times with PBS-T before addition of avidin D-horseradish peroxidase (HRP) (Vector Laboratories) diluted 1:1,000 in PBS-T-F. After a 3-h incubation at room temperature, the wells were washed 4 times with PBS-T and 4 times with PBS. Spots were developed with filtered 3-amino 9-ethylcarbazole (AEC) substrate (0.3 mg/ml AEC diluted in 0.1 M sodium acetate buffer [pH 5.0] containing a 1:1,000 dilution of 3% hydrogen peroxide). To stop the reaction, the wells were washed with water. Spots were documented and counted using an Immunospot cytotoxic T lymphocyte counter and Image Acquisition (v4.5) software (Cellular Technology). Once counted, the number of spots specific for each immunoglobulin isotype was reported as the number of either total or antigen-specific ASCs per million PBMCs.

Analysis of anti-Env IgG binding antibody responses in serum. Binding antibodies to SIVgp140 Env protein were assessed by enzyme-linked immunosorbent assay (ELISA) as described previously (59). Briefly, 96-well plates were coated overnight at 4°C with 1 μg/ml recombinant SIVmac239 or SIVsmE660 gp140 protein (Immune Technology Inc.) and then incubated with serial dilutions of heat-inactivated serum samples for 2 h followed by detection using HRP-conjugated goat anti-monkey IgG (1:10,000 dilution; Alpha Diagnostic) and 3,3,5,5-tetramethylbenzidine (TMB) substrate (KPL), followed by reading of the absorbance at 450 nm using a Bio-Tek Synergy H1 multimode microplate reader with Gen 5 (v2.0) software. A dilution series of an SIVmac239 or SIVsmE660 gp140-specific IgG standard with a known concentration was included in parallel, and antigen-specific concentrations relative to the standard were estimated and reported as the antigen-specific antibody quantity (in micrograms per milliliter).

Measurement of SIV Env-specific and total antibody in mucosal secretions. Rectal or vaginal secretions were collected by consecutively applying two premoistened Weck-Cel sponges (Beaver-Visitec, Waltham, MA) consecutively in either the rectum or vaginal vault as described previously (60). Sponges with secretions were stored at −80°C. The secretions were eluted from thawed sponges by centrifugation with 150 μl ice-cold RPMI 1640 containing 2% bovine serum albumin (BSA) and a previously described cocktail of protease inhibitors (60, 61). The concentrations of SIV gp140-specific IgA or IgG antibodies and total IgA or IgG were measured by ELISA as previously described (60), using plates coated with 100 ng per well of the above-described gp140 proteins or 250 ng per well of goat anti-monkey IgA (Alpha Diagnostics, San Antonio, TX) or IgG (MP Biomedicals). Pooled RM serum containing known amounts of Ig or SIV antibody was used as a standard. For all IgA assays, serum or secretion samples were first treated with protein G-Sepharose as described previously (60) to remove IgG. The plates were developed with biotinylated goat anti-monkey IgA (Rockland) or anti-human IgG, followed by NeutraLite avidin-peroxidase and TMB (all Southern Biotech). The concentration of anti-SIV IgA or IgG in each secretion was subsequently divided by the concentration of total IgA or IgG to obtain the specific activity (in nanograms of anti-SIV antibody per microgram of immunoglobulin). The secretion was considered positive for SIV antibody if it had a specific activity that was greater than the mean specific activity plus 3 standard deviations (SD) in secretions from naive animals. If a secretion had no detectable antibody, it was assigned the mean specific activity value for naive macaques. The concentrations of SIV-specific IgG in plasma were considered significant if they were 3.4-fold greater than the concentration measured in the animal's preimmune plasma sample.

Antibody-dependent phagocytosis (ADP). Phagocytosis assays were done as previously described (25), with the exception that the incubation time was reduced and a trypsinization step was added to remove nonphagocytosed beads stuck to cell surfaces. Briefly, 1.8×10^6 neutravidin-conjugated fluorescent beads (1-μm Fluorospheres; Invitrogen) were coated with biotinylated recombinant SIVsmE660 gp140 (Immune Technology) and then incubated for 1 h at 37°C in 5% CO_2 with 1/20 dilutions of serum in triplicate wells of a 96-well V-bottom plate. THP-1 cells (2×10^4 per well) were then added. After 4 h of incubation, the cells were washed with Ca^{2+}- and Mg^{2+}-free Dulbecco's PBS (DPBS), incubated for 10 min with 50 μl of 0.05% trypsin-EDTA (Life Technologies), washed 2× in DPBS, and then resuspended in 1% paraformaldehyde. The cells were analyzed for fluorescence by flow cytometry. The phagocytic score was calculated as described previously (25) by multiplying the number of bead-positive cells by their median fluorescent intensity. The average score for control wells containing THP-1 cells and gp140-coated beads in the absence of serum was subtracted prior to calculation of the average score for test samples.

Virus neutralization assays. Virus neutralization assays were carried out as described previously (62, 63). The SIVsmE660.11 Env pseudovirus was generated by transfecting Env-expressing plasmid DNA alongside HIV-1 SG3Δ Env proviral backbone DNA into 293T cells, using the Fugene HD reagent as recommended by the manufacturer (Promega). The pseudovirus stock was collected from the 293T cell supernatants at 48 to 72 h after transfection, clarified by centrifugation, divided into small volumes, and frozen at −80°C. The SIVsmE660 challenge virus stock was generated by combining an aliquot of the original SIVsmE660 stock (SIVsmE660-ABL; virus stock created on 12 May 2010) with multiple aliquots frozen during the M2 challenges. The titers of SIVsmE660.11 Env pseudovirus and the SIVsmE660 challenge virus were determined on TZM-bl cells. Fivefold serial dilutions of heat-inactivated serum collected at the baseline or at postimmunization time points were assayed for their inhibitory activity using the TZM-bl cells, with luciferase activity being the readout. Briefly, TZM-bl cells were plated and cultured overnight in flat-bottom 96-well plates. Pseudovirus or virus stock (2,000 IU per well) in Dulbecco modified Eagle medium with ~3.5% FBS (HyClone) was incubated with serial dilutions of test serum and added to the plated TZM-bl cells in the presence of 40 μg/ml DEAE-dextran. At 48 h postinfection, the cells were lysed, and luciferase activity was measured using a Bio-Tek Synergy HT multimode microplate reader with Gen 5 (v2.0) software. The average background luminescence for a series of uninfected wells was subtracted from the luminescence for each experimental well, and infectivity curves were generated using GraphPad Prism (v6.0) software, where the values from the test wells were compared with the value from a well containing only virus (100% infectivity). Each virus-serum combination was tested at least twice independently in duplicate wells in each experiment.

PBMC stimulation and T cell intracellular cytokine staining (ICS) assay. Blood samples were collected in 4- or 8-ml cell preparation tubes (CPTs) containing 0.1 M sodium citrate (BD Biosciences). The CPTs were centrifuged at $1,500 \times g$ without brakes for 40 min at room temperature. Plasma was collected, and mononuclear cells were separated. ACK lysis buffer (Lonza, Walkersville, MD, USA) was used to lyse residual red blood cells, and the cells were washed with PBS before counting for use. Fresh PBMCs were used in assays unless otherwise specified. RPMI 1640 medium containing 1× L-glutamine was purchased from Corning Life Sciences/MediaTech Inc., Manassas, VA. The medium was supplemented to contain a final concentration of 10% FBS (Corning Life Sciences/Media Tech Inc., Manassas, VA), 10 mM HEPES, 1× minimal essential medium nonessential amino acids (Corning Life Sciences/Media Tech Inc., Manassas, VA), 1 mM sodium pyruvate (Lonza, Walkersville, MD, USA), 1 mM penicillin-streptomycin containing amphotericin B (Sigma Life Sciences, St. Louis, MO, USA), and 1× 2-mercaptoethanol (Gibco, Invitrogen, Carlsbad, CA, USA). PBMCs were stimulated for detection of cytokine production by T cells as described before (11). Briefly, 2×10^6 cells were cultured in a 200-μl final volume in 5-ml polypropylene tubes (BD Biosciences, San Diego, CA, USA) in the presence of anti-CD28 (1 μg/ml), anti-CD49d (1 μg/ml), and the following: (i) a negative control with dimethyl sulfoxide only, (ii) a Gag peptide pool (1 to 125 peptides derived from SIVmac239) at a final concentration of 1 μg/ml, (iii) an Env peptide pool 1 (1 to 110 peptides from SIVmac239) at a final concentration of 1

μg/ml, (iv) an Env peptide pool 2 (111 to 218 peptides from SIVmac239) at a final concentration of 1 μg/ml, and (v) phorbol myristate acetate-ionomycin. Cells were cultured for 2 h before adding brefeldin A (Sigma-Aldrich, St. Louis, MO) for an additional 4 h. Cells were transferred to 4°C overnight and stained for assaying by flow cytometry. Aqua viability dye (Invitrogen, CA) was used to stain for dead cells. The following antibodies were used to stain the cells. Fluorescein isothiocyanate (FITC)-conjugated anti-human IL-2 (clone MQ1-17H12; BioLegend), phycoerythrin (PE)-conjugated anti-human CCR7 (clone 150503; R&D Systems, MN), peridinin chlorophyll protein (PerCP)-conjugated anti-human CD4 (clone OKT4; BioLegend), PE-Cy7-conjugated anti-human TNF (clone MAb11; eBioscience, CA), Pacific Blue-conjugated anti-human CD8a (clone RPA-T8; BioLegend, CA), Qdot 605-conjugated anti-human CD45RA (clone MEM-56; Invitrogen, CA), allophycocyanin (APC)-conjugated anti-human IFN-γ (clone 4S.B3; BioLegend, CA), and Alexa Fluor 700-conjugated anti-human CD3 (clone SP34-2; BD Biosciences, CA). Cells were stained for dead cells in PBS at room temperature for 30 min and washed 1 time with staining buffer (PBS containing 5% FBS). Cells were stained for CD4, CD8a, CD45Ra, and CCR7 for 30 min at room temperature and washed 2 times with staining buffer. Cells were fixed and permeabilized using Cytofix/Cytoperm buffer (BD Biosciences, CA) for 10 min at room temperature. Cells were washed with 1$\times$ Perm/Wash buffer (BD Biosciences, CA) and stained for IL-2, TNF, IFN-γ and CD3 in Perm/Wash buffer for 30 min at room temperature. Cells were washed 2 times with Perm/Wash buffer and 1 time with staining buffer and acquired using a 3-laser-powered LSR II flow cytometer (BD Biosciences, CA). Flow cytometry data were analyzed using FlowJo software (TreeStar, OR). Polyfunctional T cell responses were quantified using SPICE software (Vaccine Research Center, NIH, Bethesda, MD).

PBMC staining for analyzing innate responses by flow cytometry. PBMCs were isolated from 4-ml CPTs as described above for PBMC stimulation and T cell ICS staining. The following antibodies were used to stain the 12-color innate staining panel: FITC-conjugated anti-human CCR7 (clone 150503; R&D Systems, MN), PE-conjugated anti-human BDCA-1 (clone AD5-8E7; Miltenyi Biotech, CA), PerCP-conjugated anti-human HLA-DR (clone L243; BioLegend, CA), PE-CF594-conjugated anti-human CD3 (clone SP34-2; BD Biosciences, CA), PE-Cy7-conjugated anti-human CD123 (clone 7G3; BD Biosciences, CA), Pacific Blue-conjugated anti-human CD86 (clone IT2.2; BioLegend, CA), Aqua cell viability stain (Invitrogen, CA), Qdot 605-conjugated anti-human CD14 (clone TüK4; Invitrogen, CA), Qdot 705-conjugated anti-human CD8a (clone 3B5; Invitrogen, CA), APC-conjugated anti-human CD11c (clone S-HCL-3; BD Biosciences, CA), Alexa Fluor 700-conjugated anti-human CD16 (clone 3G8; BioLegend, CA), and APC-Cy7-conjugated anti-human CD20 (clone 2H7; BioLegend, CA). Cells were stained for dead cells for 30 min at room temperature and washed 1 time with staining buffer (PBS with 5% FBS). Antibody cocktail was prepared to stain for the surface markers mentioned above and stained in a 100-μl staining volume for 30 min at room temperature. The cells were washed 2 times with staining buffer and fixed with Cytofix (BD Biosciences, CA) for 10 min. Cells were washed 1 time with staining buffer and acquired using an LSR II flow cytometer (BD Biosciences, CA). Flow cytometry data were analyzed using FlowJo software (TreeStar, OR).

Measurement of SIV RNA plasma load. The SIV copy number was determined using a quantitative real-time PCR as previously described (64). All samples were run in duplicate, and the mean values are reported.

Microarray analyses. Total RNA from whole blood was purified from PAXgene blood RNA tubes (BD) with PAXgene blood RNA kits (Qiagen) according to the manufacturer's protocol, utilizing on-column DNase digestion according to the manufacturer's instructions. The integrity and quantity of the extracted RNA were assessed with an Agilent bioanalyzer (Agilent Technologies, Santa Clara, CA) and a NanoDrop 2000 spectrophotometer (Thermo Scientific Inc., Wilmington, DE). An Affymetrix IVT Express kit was used to amplify 250 ng of total RNA according to a modified protocol; nonspecific binding by hemoglobin transcripts was inhibited by the inclusion of a set of 5 peptide nucleic acid (PNA) oligonucleotides specific for regions of *Macaca mulatta* hemoglobin α and β (65) mRNA in the reverse transcription cocktail, as described previously (66). Samples were hybridized to Affymetrix GeneChip rhesus macaque genome arrays (Affymetrix, Santa Clara, CA), which contain over 52,000 individual probe sets that assay over 47,000 transcripts. The arrays were washed, stained, and scanned as described in the Affymetrix GeneChip expression analysis technical manual, the chips were scanned using an Affymetrix 7000G scanner, and the .cel files were extracted from the raw scanned images using Affymetrix GeneChip command console software. RNA samples were processed at all steps by a single operator in balanced blocks to minimize handling bias. RNA purification was performed in batches of 24 samples representing samples from all time points from three individual monkeys split between three vaccine groups. Hybridization was batched in groups of 42 samples that also contained samples from all time points from six animals balanced between vaccine groups and TRIM5α genotype. Data quality was assessed by use of the array quality metrics R package (67). After removal of outliers, the .cel files for all samples were grouped, and the microarray intensity data of the probe sets were normalized by robust multiarray average (RMA), which includes global background adjustment and quantile normalization. Probe sets that match the same human gene identifier were collapsed by taking the probe set with the highest level of expression across all samples (here referred to "genes"). Considering all samples, we next removed the 30% of the genes with lowest mean level of expression and the 30% of the genes with the lowest variance, leaving 9,800 genes for the subsequent analyses. Baseline-normalized expression data (here referred to "fold change") were obtained for each monkey by subtracting the value at the baseline from the corresponding value at each time point. Principal component analysis (PCA) was performed using the 5,000 genes with the highest absolute fold change across all samples. Differential expression analyses were performed for each treatment group and for each time point by comparison to the level of expression at the baseline using the limma R package (68) (adjusted *P* value by the pairwise test, $<$0.05;

mean fold change, >1.25). Gene set enrichment analysis (GSEA; default parameters; nominal *P* value, <0.05) (35) was performed using the blood transcription modules (BTMs) (36) as gene sets. The signatures of immunogenicity at each time point were defined by the Spearman correlation between fold change values and the prechallenge vaginal IgG SIVmac239 Env titers ($P < 0.01$). The signatures of protection were defined for each time point by the limma test (adjusted *P* value, <0.05; mean fold change, >1.25) between the fold change values for infected and uninfected monkeys. GSEA was performed using genes preranked by either their Spearman correlation values (immunogenicity GSEA) or their $\log_2$ fold change values (protection outcome GSEA).

TRIM5α genotyping. Genomic DNA was isolated from lymphocytes from rhesus macaques with a QIAamp DNA kit (Qiagen) and sequenced for *TRIM5α* exons.

Statistics. Multigroup comparisons for all immunological readouts were performed using the nonparametric Kruskal-Wallis test followed by the use of Dunn's correction. A log-rank Mantel-Cox test was used to compare the significance of survival curves. A Wilcoxon signed-rank paired *t* test was used to compare the significance of changes in the frequencies of PBMCs in comparison with their baseline frequencies when longitudinal studies of innate responses were performed. A nonparametric Mann-Whitney test was used to compare the immune responses in uninfected and infected animals. Spearman's correlation analysis was performed to assess the impact of immunological correlates. All analyses were performed using GraphPad Prism (v6.0) software. The *P* values determined in the study were not corrected for multiple comparisons. Note that the *P* values presented in the figures with multigroup comparisons are corrected (by the use of Dunn's *post hoc* analysis) in a manner specific to the plots but are not corrected for the entire study.

SUPPLEMENTAL MATERIAL

Supplemental material for this article may be found at https://doi.org/10.1128/JVI.01844-16.

TEXT S1, PDF file, 2.7 MB.

TEXT S2, XLSX file, 1.5 MB.

ACKNOWLEDGMENTS

We thank all animal staff at the Yerkes National Primate Research Center at Emory University, especially Christopher Souder, Robert Sheffield, Stephanie Ehnert, and Elizabeth Strobert, in helping out with the macaque study. We acknowledge Steve Bosinger, Nirav Patel, and Greg Tharp at the Yerkes Genomic Core for help with the microarray assay in the transcriptomics study. We acknowledge Benton Lawson from the CFAR Virology Core for measurement of the SIV load and Kenneth Rogers for TRIM5α genotyping. We thank Robert L. Wilson for excellent technical assistance in processing the secretions and measuring mucosal antibodies. We thank Tianwei Yu for help with statistical analysis. We thank the CFAR Immunology/Emory Vaccine Center Flow Cytometry Core. We acknowledge the NIH AIDS Reagent Program for Gag and Env peptide pool reagents.

The CFAR Immunology/Emory Vaccine Center Flow Cytometry Core is supported by an NIH grant (P30 A050509). This work was supported by grants NIH P51-RR000165 and P51-OD011132 to the Yerkes National Primate Research Center. Studies were also supported by grants P01-AI096187 (principal investigator, Eric Hunter) and R01-AI58706 (principal investigator, Cynthia A. Derdeyn) from the National Institutes of Health and a Collaboration for AIDS Vaccine Discovery (CAVD) grant (principal investigator, Bali Pulendran) from the Bill and Melinda Gates Foundation.

REFERENCES

1. Excler JL, Tomaras GD, Russell ND. 2013. Novel directions in HIV-1 vaccines revealed from clinical trials. Curr Opin HIV AIDS 8:421–431. https://doi.org/10.1097/COH.0b013e3283632c26.
2. Kim JH, Excler JL, Michael NL. 2015. Lessons from the RV144 Thai phase III HIV-1 vaccine trial and the search for correlates of protection. Annu Rev Med 66:423–437. https://doi.org/10.1146/annurev-med-052912-123749.
3. Buchbinder SP, Mehrotra DV, Duerr A, Fitzgerald DW, Mogg R, Li D, Gilbert PB, Lama JR, Marmor M, Del Rio C, McElrath MJ, Casimiro DR, Gottesdiener KM, Chodakewitz JA, Corey L, Robertson MN, Step Study Protocol Team. 2008. Efficacy assessment of a cell-mediated immunity HIV-1 vaccine (the Step Study): a double-blind, randomised, placebo-controlled, test-of-concept trial. Lancet 372:1881–1893. https://doi.org/10.1016/S0140-6736(08)61591-3.
4. Rerks-Ngarm S, Pitisuttithum P, Nitayaphan S, Kaewkungwal J, Chiu J, Paris R, Premsri N, Namwat C, de Souza M, Adams E, Benenson M, Gurunathan S, Tartaglia J, McNeil JG, Francis DP, Stablein D, Birx DL, Chunsuttiwat S, Khamboonruang C, Thongcharoen P, Robb ML, Michael NL, Kunasol P, Kim JH, MOPH-TAVEG Investigators. 2009. Vaccination with ALVAC and AIDSVAX to prevent HIV-1 infection in Thailand. N Engl J Med 361:2209–2220. https://doi.org/10.1056/NEJMoa0908492.
5. Haynes BF, Gilbert PB, McElrath MJ, Zolla-Pazner S, Tomaras GD, Alam SM, Evans DT, Montefiori DC, Karnasuta C, Sutthent R, Liao HX, DeVico AL, Lewis GK, Williams C, Pinter A, Fong Y, Janes H, DeCamp A, Huang Y, Rao M, Billings E, Karasavvas N, Robb ML, Ngauy V, de Souza MS, Paris R, Ferrari G, Bailer RT, Soderberg KA, Andrews C, Berman PW, Frahm N, De Rosa SC, Alpert MD, Yates NL, Shen X, Koup RA, Pitisuttithum P, Kaewkungwal J, Nitayaphan S, Rerks-Ngarm S, Michael NL, Kim JH. 2012.

Immune-correlates analysis of an HIV-1 vaccine efficacy trial. N Engl J Med 366:1275–1286. https://doi.org/10.1056/NEJMoa1113425.
6. Pulendran B, Ahmed R. 2006. Translating innate immunity into immunological memory: implications for vaccine development. Cell 124:849–863. https://doi.org/10.1016/j.cell.2006.02.019.
7. Pulendran B, Ahmed R. 2011. Immunological mechanisms of vaccination. Nat Immunol 12:509–517.
8. Coffman RL, Sher A, Seder RA. 2010. Vaccine adjuvants: putting innate immunity to work. Immunity 33:492–503. https://doi.org/10.1016/j.immuni.2010.10.002.
9. Wille-Reece U, Flynn BJ, Lore K, Koup RA, Kedl RM, Mattapallil JJ, Weiss WR, Roederer M, Seder RA. 2005. HIV Gag protein conjugated to a Toll-like receptor 7/8 agonist improves the magnitude and quality of Th1 and $CD8^+$ T cell responses in nonhuman primates. Proc Natl Acad Sci U S A 102:15190–15194. https://doi.org/10.1073/pnas.0507484102.
10. Francica JR, Sheng Z, Zhang Z, Nishimura Y, Shingai M, Ramesh A, Keele BF, Schmidt SD, Flynn BJ, Darko S, Lynch RM, Yamamoto T, Matus-Nicodemos R, Wolinsky D, NISC Comparative Sequencing Program, Nason M, Valiante NM, Malyala P, De Gregorio E, Barnett SW, Singh M, O'Hagan DT, Koup RA, Mascola JR, Martin MA, Kepler TB, Douek DC, Shapiro L, Seder RA. 2015. Analysis of immunoglobulin transcripts and hypermutation following SHIV(AD8) infection and protein-plus-adjuvant immunization. Nat Commun 6:6565. https://doi.org/10.1038/ncomms7565.
11. Kwissa M, Amara RR, Robinson HL, Moss B, Alkan S, Jabbar A, Villinger F, Pulendran B. 2007. Adjuvanting a DNA vaccine with a TLR9 ligand plus Flt3 ligand results in enhanced cellular immunity against the simian immunodeficiency virus. J Exp Med 204:2733–2746. https://doi.org/10.1084/jem.20071211.
12. Napolitani G, Rinaldi A, Bertoni F, Sallusto F, Lanzavecchia A. 2005. Selected Toll-like receptor agonist combinations synergistically trigger a T helper type 1-polarizing program in dendritic cells. Nat Immunol 6:769–776. https://doi.org/10.1038/ni1223.
13. Kasturi SP, Skountzou I, Albrecht RA, Koutsonanos D, Hua T, Nakaya HI, Ravindran R, Stewart S, Alam M, Kwissa M, Villinger F, Murthy N, Steel J, Jacob J, Hogan RJ, Garcia-Sastre A, Compans R, Pulendran B. 2011. Programming the magnitude and persistence of antibody responses with innate immunity. Nature 470:543–547. https://doi.org/10.1038/nature09737.
14. Bachmann MF, Odermatt B, Hengartner H, Zinkernagel RM. 1996. Induction of long-lived germinal centers associated with persisting antigen after viral infection. J Exp Med 183:2259–2269. https://doi.org/10.1084/jem.183.5.2259.
15. Fox CB, Sivananthan SJ, Duthie MS, Vergara J, Guderian JA, Moon E, Coblentz D, Reed SG, Carter D. 2014. A nanoliposome delivery system to synergistically trigger TLR4 and TLR7. J Nanobiotechnol 12:17. https://doi.org/10.1186/1477-3155-12-17.
16. Goff PH, Hayashi T, Martinez-Gil L, Corr M, Crain B, Yao S, Cottam HB, Chan M, Ramos I, Eggink D, Heshmati M, Krammer F, Messer K, Pu M, Fernandez-Sesma A, Palese P, Carson DA. 2015. Synthetic Toll-like receptor 4 (TLR4) and TLR7 ligands as influenza virus vaccine adjuvants induce rapid, sustained, and broadly protective responses. J Virol 89:3221–3235. https://doi.org/10.1128/JVI.03337-14.
17. McKay PF, King DF, Mann JF, Barinaga G, Carter D, Shattock RJ. 2016. TLR4 and TLR7/8 adjuvant combinations generate different vaccine antigen-specific immune outcomes in minipigs when administered via the ID or IN routes. PLoS One 11:e0148984. https://doi.org/10.1371/journal.pone.0148984.
18. Hammonds J, Chen X, Zhang X, Lee F, Spearman P. 2007. Advances in methods for the production, purification, and characterization of HIV-1 Gag-Env pseudovirion vaccines. Vaccine 25:8036–8048. https://doi.org/10.1016/j.vaccine.2007.09.016.
19. Hicar MD, Chen X, Briney B, Hammonds J, Wang JJ, Kalams S, Spearman PW, Crowe JE, Jr. 2010. Pseudovirion particles bearing native HIV envelope trimers facilitate a novel method for generating human neutralizing monoclonal antibodies against HIV. J Acquir Immune Defic Syndr 54:223–235. https://doi.org/10.1097/QAI.0b013e3181dc98a3.
20. Vecchi S, Bufali S, Skibinski DA, O'Hagan DT, Singh M. 2012. Aluminum adjuvant dose guidelines in vaccine formulation for preclinical evaluations. J Pharm Sci 101:17–20. https://doi.org/10.1002/jps.22759.
21. Institute for Vaccine Safety. 2016. Excipients V. Institute for Vaccine Safety, Johns Hopkins Bloomberg School of Public Health, Baltimore, MD. http://www.vaccinesafety.edu/components-Excipients.htm.
22. Monie A, Hung CF, Roden R, Wu TC. 2008. Cervarix: a vaccine for the prevention of HPV 16, 18-associated cervical cancer. Biologics 2:97–105.
23. Ackerman ME, Dugast AS, Alter G. 2012. Emerging concepts on the role of innate immunity in the prevention and control of HIV infection. Annu Rev Med 63:113–130. https://doi.org/10.1146/annurev-med-050310-085221.
24. Robinson HL. 2013. Non-neutralizing antibodies in prevention of HIV infection. Expert Opin Biol Ther 13:197–207. https://doi.org/10.1517/14712598.2012.743527.
25. Ackerman ME, Moldt B, Wyatt RT, Dugast AS, McAndrew E, Tsoukas S, Jost S, Berger CT, Sciaranghella G, Liu Q, Irvine DJ, Burton DR, Alter G. 2011. A robust, high-throughput assay to determine the phagocytic activity of clinical antibody samples. J Immunol Methods 366:8–19. https://doi.org/10.1016/j.jim.2010.12.016.
26. Wrammert J, Smith K, Miller J, Langley WA, Kokko K, Larsen C, Zheng NY, Mays I, Garman L, Helms C, James J, Air GM, Capra JD, Ahmed R, Wilson PC. 2008. Rapid cloning of high-affinity human monoclonal antibodies against influenza virus. Nature 453:667–671. https://doi.org/10.1038/nature06890.
27. Silveira EL, Kasturi SP, Kovalenkov Y, Rasheed AU, Yeiser P, Jinnah ZS, Legere TH, Pulendran B, Villinger F, Wrammert J. 2015. Vaccine-induced plasmablast responses in rhesus macaques: phenotypic characterization and a source for generating antigen-specific monoclonal antibodies. J Immunol Methods 416:69–83. https://doi.org/10.1016/j.jim.2014.11.003.
28. Slifka MK, Antia R, Whitmire JK, Ahmed R. 1998. Humoral immunity due to long-lived plasma cells. Immunity 8:363–372. https://doi.org/10.1016/S1074-7613(00)80541-5.
29. Lopalco L, Bomsel M. 2011. Protecting the initial site of viral entry: an alternative HIV vaccine target. Expert Rev Vaccines 10:1253–1256. https://doi.org/10.1586/erv.11.98.
30. Sui Y, Gordon S, Franchini G, Berzofsky JA. 2013. Nonhuman primate models for HIV/AIDS vaccine development. Curr Protoc Immunol Chapter 102:Unit 12.14. https://doi.org/10.1002/0471142735.im1214s102.
31. Lai L, Kwa S, Kozlowski PA, Montefiori DC, Ferrari G, Johnson WE, Hirsch V, Villinger F, Chennareddi L, Earl PL, Moss B, Amara RR, Robinson HL. 2011. Prevention of infection by a granulocyte-macrophage colony-stimulating factor co-expressing DNA/modified vaccinia Ankara simian immunodeficiency virus vaccine. J Infect Dis 204:164–173. https://doi.org/10.1093/infdis/jir199.
32. Letvin NL, Rao SS, Montefiori DC, Seaman MS, Sun Y, Lim SY, Yeh WW, Asmal M, Gelman RS, Shen L, Whitney JB, Seoighe C, Lacerda M, Keating S, Norris PJ, Hudgens MG, Gilbert PB, Buzby AP, Mach LV, Zhang J, Balachandran H, Shaw GM, Schmidt SD, Todd JP, Dodson A, Mascola JR, Nabel GJ. 2011. Immune and genetic correlates of vaccine protection against mucosal infection by SIV in monkeys. Sci Transl Med 3:81ra36. https://doi.org/10.1126/scitranslmed.3002351.
33. Kwissa M, Nakaya HI, Oluoch H, Pulendran B. 2012. Distinct TLR adjuvants differentially stimulate systemic and local innate immune responses in nonhuman primates. Blood 119:2044–2055. https://doi.org/10.1182/blood-2011-10-388579.
34. Querec TD, Akondy RS, Lee EK, Cao W, Nakaya HI, Teuwen D, Pirani A, Gernert K, Deng J, Marzolf B, Kennedy K, Wu H, Bennouna S, Oluoch H, Miller J, Vencio RZ, Mulligan M, Aderem A, Ahmed R, Pulendran B. 2009. Systems biology approach predicts immunogenicity of the yellow fever vaccine in humans. Nat Immunol 10:116–125. https://doi.org/10.1038/ni.1688.
35. Subramanian A, Tamayo P, Mootha VK, Mukherjee S, Ebert BL, Gillette MA, Paulovich A, Pomeroy SL, Golub TR, Lander ES, Mesirov JP. 2005. Gene set enrichment analysis: a knowledge-based approach for interpreting genome-wide expression profiles. Proc Natl Acad Sci U S A 102:15545–15550. https://doi.org/10.1073/pnas.0506580102.
36. Li S, Rouphael N, Duraisingham S, Romero-Steiner S, Presnell S, Davis C, Schmidt DS, Johnson SE, Milton A, Rajam G, Kasturi S, Carlone GM, Quinn C, Chaussabel D, Palucka AK, Mulligan MJ, Ahmed R, Stephens DS, Nakaya HI, Pulendran B. 2014. Molecular signatures of antibody responses derived from a systems biology study of five human vaccines. Nat Immunol 15:195–204. https://doi.org/10.1038/ni.2789.
37. Sundling C, Forsell MN, O'Dell S, Feng Y, Chakrabarti B, Rao SS, Lore K, Mascola JR, Wyatt RT, Douagi I, Karlsson Hedestam GB. 2010. Soluble HIV-1 Env trimers in adjuvant elicit potent and diverse functional B cell responses in primates. J Exp Med 207:2003–2017. https://doi.org/10.1084/jem.20100025.
38. Kannanganat S, Nigam P, Velu V, Earl PL, Lai L, Chennareddi L, Lawson B, Wilson RL, Montefiori DC, Kozlowski PA, Moss B, Robinson HL, Amara

RR. 2010. Preexisting vaccinia virus immunity decreases SIV-specific cellular immunity but does not diminish humoral immunity and efficacy of a DNA/MVA vaccine. J Immunol 185:7262–7273. https://doi.org/10.4049/jimmunol.1000751.
39. Xiao P, Patterson LJ, Kuate S, Brocca-Cofano E, Thomas MA, Venzon D, Zhao J, DiPasquale J, Fenizia C, Lee EM, Kalisz I, Kalyanaraman VS, Pal R, Montefiori D, Keele BF, Robert-Guroff M. 2012. Replicating adenovirus-simian immunodeficiency virus (SIV) recombinant priming and envelope protein boosting elicits localized, mucosal IgA immunity in rhesus macaques correlated with delayed acquisition following a repeated low-dose rectal SIV(mac251) challenge. J Virol 86:4644–4657. https://doi.org/10.1128/JVI.06812-11.
40. Jensen K, Nabi R, Van Rompay KKA, Robichaux S, Lifson JD, Piatak M, Jacobs WR, Fennelly G, Canfield D, Mollan KR, Hudgens MG, Larsen MH, Amedee AM, Kozlowski PA, De Paris K. 2016. Vaccine-elicited mucosal and systemic antibody responses are associated with reduced simian immunodeficiency viremia in infant macaques. J Virol 90:7285–7302. https://doi.org/10.1128/JVI.00481-16.
41. Bomsel M, Tudor D, Drillet AS, Alfsen A, Ganor Y, Roger MG, Mouz N, Amacker M, Chalifour A, Diomede L, Devillier G, Cong Z, Wei Q, Gao H, Qin C, Yang GB, Zurbriggen R, Lopalco L, Fleury S. 2011. Immunization with HIV-1 gp41 subunit virosomes induces mucosal antibodies protecting nonhuman primates against vaginal SHIV challenges. Immunity 34:269–280. https://doi.org/10.1016/j.immuni.2011.01.015.
42. Lai L, Vodros D, Kozlowski PA, Montefiori DC, Wilson RL, Akerstrom VL, Chennareddi L, Yu T, Kannanganat S, Ofielu L, Villinger F, Wyatt LS, Moss B, Amara RR, Robinson HL. 2007. GM-CSF DNA: an adjuvant for higher avidity IgG, rectal IgA, and increased protection against the acute phase of a SHIV-89.6P challenge by a DNA/MVA immunodeficiency virus vaccine. Virology 369:153–167. https://doi.org/10.1016/j.virol.2007.07.017.
43. Burton DR, Hessell AJ, Keele BF, Klasse PJ, Ketas TA, Moldt B, Dunlop DC, Poignard P, Doyle LA, Cavacini L, Veazey RS, Moore JP. 2011. Limited or no protection by weakly or nonneutralizing antibodies against vaginal SHIV challenge of macaques compared with a strongly neutralizing antibody. Proc Natl Acad Sci U S A 108:11181–11186. https://doi.org/10.1073/pnas.1103012108.
44. Moldt B, Le KM, Carnathan DG, Whitney JB, Schultz N, Lewis MG, Borducchi EN, Smith KM, Mackel JJ, Sweat SL, Hodges AP, Godzik A, Parren PW, Silvestri G, Barouch DH, Burton DR. 2016. Neutralizing antibody affords comparable protection against vaginal and rectal simian/human immunodeficiency virus challenge in macaques. AIDS 30:1543–1551. https://doi.org/10.1097/QAD.0000000000001102.
45. Gautam R, Nishimura Y, Pegu A, Nason MC, Klein F, Gazumyan A, Golijanin J, Buckler-White A, Sadjadpour R, Wang K, Mankoff Z, Schmidt SD, Lifson JD, Mascola JR, Nussenzweig MC, Martin MA. 2016. A single injection of anti-HIV-1 antibodies protects against repeated SHIV challenges. Nature 533:105–109. https://doi.org/10.1038/nature17677.
46. Santra S, Tomaras GD, Warrier R, Nicely NI, Liao HX, Pollara J, Liu P, Alam SM, Zhang R, Cocklin SL, Shen X, Duffy R, Xia SM, Schutte RJ, Pemble CW, IV, Dennison SM, Li H, Chao A, Vidnovic K, Evans A, Klein K, Kumar A, Robinson J, Landucci G, Forthal DN, Montefiori DC, Kaewkungwal J, Nitayaphan S, Pitisuttithum P, Rerks-Ngarm S, Robb ML, Michael NL, Kim JH, Soderberg KA, Giorgi EE, Blair L, Korber BT, Moog C, Shattock RJ, Letvin NL, Schmitz JE, Moody MA, Gao F, Ferrari G, Shaw GM, Haynes BF. 2015. Human non-neutralizing HIV-1 envelope monoclonal antibodies limit the number of founder viruses during SHIV mucosal infection in rhesus macaques. PLoS Pathog 11:e1005042. https://doi.org/10.1371/journal.ppat.1005042.
47. Moog C, Dereuddre-Bosquet N, Teillaud JL, Biedma ME, Holl V, Van Ham G, Heyndrickx L, Van Dorsselaer A, Katinger D, Vcelar B, Zolla-Pazner S, Mangeot I, Kelly C, Shattock RJ, Le Grand R. 2014. Protective effect of vaginal application of neutralizing and nonneutralizing inhibitory antibodies against vaginal SHIV challenge in macaques. Mucosal Immunol 7:46–56. https://doi.org/10.1038/mi.2013.23.
48. Sholukh AM, Watkins JD, Vyas HK, Gupta S, Lakhashe SK, Thorat S, Zhou M, Hemashettar G, Bachler BC, Forthal DN, Villinger F, Sattentau QJ, Weiss RA, Agatic G, Corti D, Lanzavecchia A, Heeney JL, Ruprecht RM. 2015. Defense-in-depth by mucosally administered anti-HIV dimeric IgA2 and systemic IgG1 mAbs: complete protection of rhesus monkeys from mucosal SHIV challenge. Vaccine 33:2086–2095. https://doi.org/10.1016/j.vaccine.2015.02.020.
49. Altfeld M, Gale M, Jr. 2015. Innate immunity against HIV-1 infection. Nat Immunol 16:554–562. https://doi.org/10.1038/ni.3157.
50. Kwa S, Lai L, Gangadhara S, Siddiqui M, Pillai VB, Labranche C, Yu T, Moss B, Montefiori DC, Robinson HL, Kozlowski PA, Amara RR. 2014. CD40L-adjuvanted DNA/modified vaccinia virus Ankara simian immunodeficiency virus SIV239 vaccine enhances SIV-specific humoral and cellular immunity and improves protection against a heterologous SIVE660 mucosal challenge. J Virol 88:9579–9589. https://doi.org/10.1128/JVI.00975-14.
51. Barouch DH, Liu J, Li H, Maxfield LF, Abbink P, Lynch DM, Iampietro MJ, SanMiguel A, Seaman MS, Ferrari G, Forthal DN, Ourmanov I, Hirsch VM, Carville A, Mansfield KG, Stablein D, Pau MG, Schuitemaker H, Sadoff JC, Billings EA, Rao M, Robb ML, Kim JH, Marovich MA, Goudsmit J, Michael NL. 2012. Vaccine protection against acquisition of neutralization-resistant SIV challenges in rhesus monkeys. Nature 482:89–93. https://doi.org/10.1038/nature10766.
52. Barouch DH, Stephenson KE, Borducchi EN, Smith K, Stanley K, McNally AG, Liu J, Abbink P, Maxfield LF, Seaman MS, Dugast AS, Alter G, Ferguson M, Li W, Earl PL, Moss B, Giorgi EE, Szinger JJ, Eller LA, Billings EA, Rao M, Tovanabutra S, Sanders-Buell E, Weijtens M, Pau MG, Schuitemaker H, Robb ML, Kim JH, Korber BT, Michael NL. 2013. Protective efficacy of a global HIV-1 mosaic vaccine against heterologous SHIV challenges in rhesus monkeys. Cell 155:531–539. https://doi.org/10.1016/j.cell.2013.09.061.
53. Barouch DH, Alter G, Broge T, Linde C, Ackerman ME, Brown EP, Borducchi EN, Smith KM, Nkolola JP, Liu J, Shields J, Parenteau L, Whitney JB, Abbink P, Ng'ang'a DM, Seaman MS, Lavine CL, Perry JR, Li W, Colantonio AD, Lewis MG, Chen B, Wenschuh H, Reimer U, Piatak M, Lifson JD, Handley SA, Virgin HW, Koutsoukos M, Lorin C, Voss G, Weijtens M, Pau MG, Schuitemaker H. 2015. HIV-1 vaccines. Protective efficacy of adenovirus/protein vaccines against SIV challenges in rhesus monkeys. Science 349:320–324. https://doi.org/10.1126/science.aab3886.
54. Tuero I, Mohanram V, Musich T, Miller L, Vargas-Inchaustegui DA, Demberg T, Venzon D, Kalisz I, Kalyanaraman VS, Pal R, Ferrari MG, LaBranche C, Montefiori DC, Rao M, Vaccari M, Franchini G, Barnett SW, Robert-Guroff M. 2015. Mucosal B cells are associated with delayed SIV acquisition in vaccinated female but not male rhesus macaques following SIVmac251 rectal challenge. PLoS Pathog 11:e1005101. https://doi.org/10.1371/journal.ppat.1005101.
55. Vaccari M, Gordon SN, Fourati S, Schifanella L, Liyanage NP, Cameron M, Keele BF, Shen X, Tomaras GD, Billings E, Rao M, Chung AW, Dowell KG, Bailey-Kellogg C, Brown EP, Ackerman ME, Vargas-Inchaustegui DA, Whitney S, Doster MN, Binello N, Pegu P, Montefiori DC, Foulds K, Quinn DS, Donaldson M, Liang F, Lore K, Roederer M, Koup RA, McDermott A, Ma ZM, Miller CJ, Phan TB, Forthal DN, Blackburn M, Caccuri F, Bissa M, Ferrari G, Kalyanaraman V, Ferrari MG, Thompson D, Robert-Guroff M, Ratto-Kim S, Kim JH, Michael NL, Phogat S, Barnett SW, Tartaglia J, Venzon D, Stablein DM, Alter G, Sekaly RP, Franchini G. 2016. Adjuvant-dependent innate and adaptive immune signatures of risk of SIV acquisition. Nat Med 22:762–770. https://doi.org/10.1038/nm.4105.
56. Kwissa M, Nakaya HI, Onlamoon N, Wrammert J, Villinger F, Perng GC, Yoksan S, Pattanapanyasat K, Chokephaibulkit K, Ahmed R, Pulendran B. 2014. Dengue virus infection induces expansion of a CD14(+)CD16(+) monocyte population that stimulates plasmablast differentiation. Cell Host Microbe 16:115–127. https://doi.org/10.1016/j.chom.2014.06.001.
57. Reynolds MR, Sacha JB, Weiler AM, Borchardt GJ, Glidden CE, Sheppard NC, Norante FA, Castrovinci PA, Harris JJ, Robertson HT, Friedrich TC, McDermott AB, Wilson NA, Allison DB, Koff WC, Johnson WE, Watkins DI. 2011. The TRIM5{alpha} genotype of rhesus macaques affects acquisition of simian immunodeficiency virus SIVsmE660 infection after repeated limiting-dose intrarectal challenge. J Virol 85:9637–9640. https://doi.org/10.1128/JVI.05074-11.
58. Smith K, Garman L, Wrammert J, Zheng NY, Capra JD, Ahmed R, Wilson PC. 2009. Rapid generation of fully human monoclonal antibodies specific to a vaccinating antigen. Nat Protoc 4:372–384. https://doi.org/10.1038/nprot.2009.3.
59. Xiao P, Zhao J, Patterson LJ, Brocca-Cofano E, Venzon D, Kozlowski PA, Hidajat R, Demberg T, Robert-Guroff M. 2010. Multiple vaccine-elicited nonneutralizing antienvelope antibody activities contribute to protective efficacy by reducing both acute and chronic viremia following simian/human immunodeficiency virus SHIV89.6P challenge in rhesus macaques. J Virol 84:7161–7173. https://doi.org/10.1128/JVI.00410-10.
60. Kozlowski PA, Lynch RM, Patterson RR, Cu-Uvin S, Flanigan TP, Neutra MR. 2000. Modified wick method using Weck-Cel sponges for collection of human rectal secretions and analysis of mucosal HIV antibody. J Acquir Immune Defic Syndr 24:297–309.
61. Manrique M, Kozlowski PA, Cobo-Molinos A, Wang SW, Wilson RL,

Montefiori DC, Carville A, Aldovini A. 2013. Immunogenicity of a vaccine regimen composed of simian immunodeficiency virus DNA, rMVA, and viral particles administered to female rhesus macaques via four different mucosal routes. J Virol 87:4738–4750. https://doi.org/10.1128/JVI.03531-12.

62. Burton SL, Kilgore KM, Smith SA, Reddy S, Hunter E, Robinson HL, Silvestri G, Amara RR, Derdeyn CA. 2015. Breakthrough of SIV strain smE660 challenge in SIV strain mac239-vaccinated rhesus macaques despite potent autologous neutralizing antibody responses. Proc Natl Acad Sci U S A 112:10780–10785. https://doi.org/10.1073/pnas.1509731112.
63. Kilgore KM, Murphy MK, Burton SL, Wetzel KS, Smith SA, Xiao P, Reddy S, Francella N, Sodora DL, Silvestri G, Cole KS, Villinger F, Robinson JE, Pulendran B, Hunter E, Collman RG, Amara RR, Derdeyn CA. 2015. Characterization and implementation of a diverse simian immunodeficiency virus SIVsm envelope panel in the assessment of neutralizing antibody breadth elicited in rhesus macaques by multimodal vaccines expressing the SIVmac239 envelope. J Virol 89:8130–8151. https://doi.org/10.1128/JVI.01221-14.
64. Amara RR, Villinger F, Altman JD, Lydy SL, O'Neil SP, Staprans SI, Montefiori DC, Xu Y, Herndon JG, Wyatt LS, Candido MA, Kozyr NL, Earl PL, Smith JM, Ma HL, Grimm BD, Hulsey ML, Miller J, McClure HM, McNicholl JM, Moss B, Robinson HL. 2001. Control of a mucosal challenge and prevention of AIDS by a multiprotein DNA/MVA vaccine. Science 292:69–74. https://doi.org/10.1126/science.1058915.
65. Bosinger SE, Li Q, Gordon SN, Klatt NR, Duan L, Xu L, Francella N, Sidahmed A, Smith AJ, Cramer EM, Zeng M, Masopust D, Carlis JV, Ran L, Vanderford TH, Paiardini M, Isett RB, Baldwin DA, Else JG, Staprans SI, Silvestri G, Haase AT, Kelvin DJ. 2009. Global genomic analysis reveals rapid control of a robust innate response in SIV-infected sooty mangabeys. J Clin Invest 119:3556–3572. https://doi.org/10.1172/JCI40115.
66. Taaffe JE, Bosinger SE, Del Prete GQ, Else JG, Ratcliffe S, Ward CD, Migone T, Paiardini M, Silvestri G. 2012. CCR5 blockade is well tolerated and induces changes in the tissue distribution of $CCR5^+$ and $CD25^+$ T cells in healthy, SIV-uninfected rhesus macaques. J Med Primatol 41:24–42. https://doi.org/10.1111/j.1600-0684.2011.00521.x.
67. Kauffmann A, Gentleman R, Huber W. 2009. arrayQualityMetrics—a bioconductor package for quality assessment of microarray data. Bioinformatics 25:415–416. https://doi.org/10.1093/bioinformatics/btn647.
68. Ritchie ME, Phipson B, Wu D, Hu Y, Law CW, Shi W, Smyth GK. 2015. limma powers differential expression analyses for RNA-sequencing and microarray studies. Nucleic Acids Res 43:e47. https://doi.org/10.1093/nar/gkv007.